MISSOURI S&T

Missouri University of Science and Technology

Scholars' Mine

Electrical and Computer Engineering Faculty Research & Creative Works

Electrical and Computer Engineering

01 Apr 2009

Neural Network Control of Mobile Robot Formations Using RISE Feedback

Jagannathan Sarangapani
Missouri University of Science and Technology, sarangap@mst.edu

Travis Alan Dierks

Follow this and additional works at: https://scholarsmine.mst.edu/ele_comeng_facwork

🥇 Part of the Computer Sciences Commons, Electrical and Computer Engineering Commons, and the Operations Research, Systems Engineering and Industrial Engineering Commons

Neural Network Control of Mobile Robot Formations Using RISE Feedback

Travis Dierks, *Student Member, IEEE*, and S. Jagannathan, *Senior Member, IEEE*

Abstract—In this paper, an asymptotically stable (AS) combined kinematic/torque control law is developed for leader–follower-based formation control using backstepping in order to accommodate the complete dynamics of the robots and the formation, and a neural network (NN) is introduced along with robust integral of the sign of the error feedback to approximate the dynamics of the follower as well as its leader using online weight tuning. It is shown using Lyapunov theory that the errors for the entire formation are AS and that the NN weights are bounded as opposed to uniformly ultimately bounded stability which is typical with most NN controllers. Additionally, the stability of the formation in the presence of obstacles is examined using Lyapunov methods, and by treating other robots in the formation as obstacles, collisions within the formation do not occur. The asymptotic stability of the follower robots as well as the entire formation during an obstacle avoidance maneuver is demonstrated using Lyapunov methods, and numerical results are provided to verify the theoretical conjectures.

Index Terms—Formation control, kinematic/dynamic controller, Lyapunov method, neural network (NN), robust integral of the sign of the error (RISE).

I. INTRODUCTION

FOR COMPLEX tasks like search and rescue operations, mapping unknown or hazardous environments, ensuring security, and bomb sniffing, a team of robots working together offers many advantages over employing a single robot. Recognizing these benefits, robotic formation control has become the focus of many research efforts [1]–[18], and several different approaches to the problem have been proposed including behavior based, generalized coordinates, virtual structures, and leader–follower, to name a few [1]. Separation–separation and separation–bearing [2], [3] are two popular techniques in leader–follower formation control, and in this work, the latter will be considered, where the followers stay at specified separation and bearing from its designated leader.

Many formation control works [2]–[7] have proposed kinematic-based control laws to keep the formation. Thus, perfect velocity tracking assumptions are required to ensure that the desired formation is achieved as well as guarantee the stability of the formation. Therefore, numerous works [8]–[16] have proposed solution to formation control problem, which include the robot dynamics. In [8], a neural network (NN) is introduced to learn the dynamics of the follower robots. The works in [9], [10], and [11] propose decentralized approaches based on virtual points, potential functions, and the abilities of the individual robots, respectively; however, in each case, only the inertial matrix of the robots is considered, and dynamics like the centripetal and Coriolis matrix and the friction vector are ignored. In [12], a centralized control scheme is developed, and a PD controller is proposed to ensure velocity tracking; however, the derivative of the control velocity is neglected. Alternatively, the work in [13] proposes a dynamical control scheme for leader–follower-based formation control which considers the dynamics of the robots and guarantees that collisions do not occur among them. However, this control scheme is derived using potential as well as bump functions which must be at least three times differentiable. In each of these works [8]–[13], the dynamics of the follower robots are considered, whereas the effect of the dynamics of the leader on the follower (formation dynamics) is still ignored.

Our previous work [14] demonstrated that the dynamics of the lead robot are incorporated into the torque control inputs of the follower robots through the derivative of the follower's kinematic control velocity which was found to be a function of its leader's velocity. Consequently, in a formation of robots where a follower robot follows another robot directly in front of it, by considering its leader's dynamics, a robot inherently considers the dynamics of the robots in front of them. The dynamical extension in [14] provided a rigorous method of taking into account specific robot and formation dynamics; however, the dynamics of each robot were considered known. Therefore, in our previous work [15], an NN was introduced to learn the unknown dynamics of each robot as well as the dynamics of its respective leader, and the formation errors were shown to be uniformly ultimately bounded (UUB) [20].

By contrast, the contribution of this paper lies in a new asymptotically stable (AS) NN torque control law using an NN combined with the recently developed robust integral of sign of the error (RISE) feedback method originating in [18] and referred to as RISE feedback in [19]. The asymptotic stability of the entire formation, as well as the boundedness of the NN weights, is shown using Lyapunov methods as opposed to UUB, a result that is common in the NN control literature [15], [20]. The RISE method [19] is designed to reject bounded unmodeled disturbances, like NN functional reconstruction errors, to yield asymptotic tracking. An approach to blend a multilayer NN with RISE feedback for a single rigid robot control is taken in [19] where the boundedness of the actual NN weights is shown separately using the projection algorithm, while the

convergence of the tracking errors is then demonstrated by using constant controller gains. Selection of the predefined convex set in the projection algorithm to prevent the NN weights from diverging is a challenging task since the convex set must be carefully chosen to contain the ideal weights.

By contrast, in this paper, a novel weight tuning is used instead of the projection algorithm [19], and the constant bounds and gains in [19] are replaced here for formation control with time-varying functions, allowing bounds and gains to be determined with more certainty. Furthermore, Lyapunov analysis is presented to show the asymptotic convergence of the tracking errors and the boundedness of the NN weights simultaneously. The bounds and gains developed here are also applicable to single rigid robot control [19] besides formation control.

Finally, it is shown that the proposed formation controller achieves stability even in the presence of obstacles by integrating the RISE method into a simple but effective obstacle avoidance scheme which allows each follower robot to navigate around obstacles while simultaneously tracking its leader. When an obstacle is encountered, the desired separation and bearing of the follower robot are modified so that the follower navigates around the obstacle. Similar to that in [13], collisions within the formation are also avoided in this work but without the need of the additional assumption that higher order derivatives are available. Other works that have considered the formation in the presence of obstacles include [8] and [10] where potential functions were utilized. Additionally, the concept of potential trenches was applied in [16], whereas the dynamic window approach was utilized [17]. Therefore, the contributions of this manuscript include the following: 1) development of a novel formation control law by incorporating the dynamics of the leader, follower, and formation; 2) proof of asymptotic stability using Lyapunov stability even with the use of NN for approximating the leader and follower dynamics and their interactions; and 3) simplified scheme to avoid collisions among the robots and with obstacles.

This paper is organized as follows. First, in Section II, the leader–follower formation control problem is introduced, and required background information is presented. Then, the NN/RISE feedback control law is developed for the follower robots as well as the formation leader, and the stability of the overall formation is presented along with a general formation controller structure. In Section III, a leader–follower obstacle avoidance scheme is developed, and Section IV presents numerical simulations. Section V provides some concluding remarks.

II. LEADER–FOLLOWER FORMATION CONTROL

Background information on leader–follower formation control is introduced next. Throughout the development, follower robots will be denoted with a subscript "j," while the leader will be denoted by the subscript "i." The goal of separation–bearing formation control is to find a velocity control input such that

$$\lim_{t\to\infty}(L_{ijd} - L_{ij}) = 0 \quad \lim_{t\to\infty}(\Psi_{ijd} - \Psi_{ij}) = 0 \quad (1)$$

where L_{ij} and Ψ_{ij} are obtained using local sensory information and denote the measured separation and bearing of the follower j with respect to leader i, while L_{ijd} and Ψ_{ijd} represent the
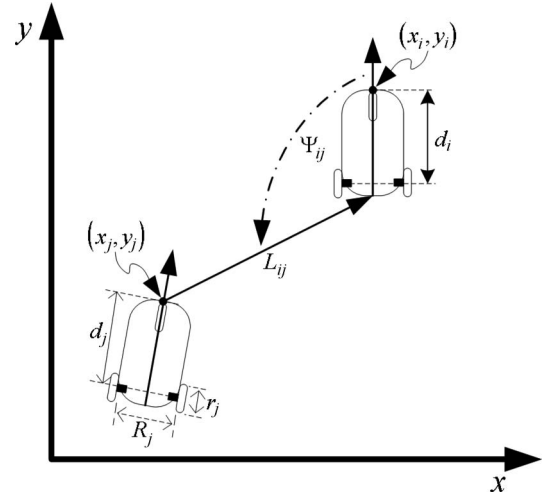

Fig. 1. Separation–bearing formation control.

desired distance and angles, respectively [2], [3], as shown in Fig. 1.

The kinematic equations for the front of the jth follower robot, (x_j, y_j), can be written as

$$\dot{q}_j = \begin{bmatrix} \dot{x}_j \\ \dot{y}_j \\ \dot{\theta}_j \end{bmatrix} = \begin{bmatrix} \cos\theta_j & -d_j\sin\theta_j \\ \sin\theta_j & d_j\cos\theta_j \\ 0 & 1 \end{bmatrix} \begin{bmatrix} v_j \\ \omega_j \end{bmatrix} = S_j(q_j)\overline{v}_j \quad (2)$$

where d_j is the distance from the rear axle to the front of the robot; $q_j = [x_j \quad y_j \quad \theta_j]^{\mathrm{T}}$ denotes the actual Cartesian position for the front of the robot and orientation, respectively; v_j and ω_j represent the linear and angular velocities, respectively; and $\overline{v}_j = [v_j \quad \omega_j]^{\mathrm{T}}$. Many robotic systems can be characterized as a system having an n-dimensional configuration space $\mathcal{C}$ with generalized coordinates $(q_1, \ldots, q_n)$ subject to ℓ constraints [23]. Applying the transformation [23], the dynamics of the mobile robots are given by

$$\overline{M}_j\dot{\overline{v}}_j + \overline{V}_{mj}(q_j, \dot{q}_j)\overline{v}_j + \overline{F}_j(\overline{v}_j) + \overline{\tau}_{dj} = \overline{\tau}_j \quad (3)$$

where $\overline{M}_j \in \Re^{\rho\times\rho}$ is a constant positive-definite inertia matrix, $\overline{V}_{mj} \in \Re^{\rho\times\rho}$ is the bounded centripetal and Coriolis matrix, $\overline{F}_j \in \Re^\rho$ is the friction vector, $\overline{\tau}_{dj} \in \Re^\rho$ represents the unknown bounded disturbances such that $\|\overline{\tau}_{dj}\| \le d_M$ and $\|[\dot{\overline{\tau}}_d^T \ddot{\overline{\tau}}_d^T]\| \le d'_M$ for known constants d_M and d'_M, $\overline{B}_j \in \Re^{\rho\times\rho}$ is a constant nonsingular input transformation matrix, $\overline{\tau}_j = \overline{B}_j\tau_j \in \Re^\rho$ is the input vector, and $\tau_j \in \Re^\rho$ is the control torque vector. For complete details on (3) and the parameters that comprise it, see [23]. It should be noted that for the nonholonomic system of (2) and (3) with n generalized coordinates q, ℓ independent constraints, and ρ actuators, the number of actuators is equal to $n - \ell$, and for this work, $n = 3$, $\ell = 1$, and $\rho = 2$. We will also apply the assumption from [23] that the linear and angular velocities are bounded for all time t.

A. Backstepping Controller Design

The complete description of the behavior of a mobile robot is given by (2) and (3). The NN/RISE controller is introduced so that the specific torque $\overline{\tau}_j(t)$ may be calculated so that

(2) and (3) exhibit the desired behavior for a given control velocity $v_{jc}(t)$ without knowing the complete dynamics of the formation.

In this paper, a two-layer NN consisting of one layer of randomly assigned constant weights $V \in \Re^{axL}$ in the input layer and one layer of tunable weights $W \in \Re^{Lxb}$ in the output layer, with a inputs, b outputs, and L hidden neurons, is considered. The *universal approximation property* for NN [20] states that for any smooth function $f(x)$, there exists an NN such that $f(x) = W^T \sigma(V^T x) + \varepsilon$ for some ideal weights W, V, where ε is the NN functional approximation error and $\sigma(\cdot) : \Re^L \to \Re^L$ is the activation function in the hidden layers. It has been shown that by randomly selecting the input layer weights V, the activation function $\sigma(\overline{x}) = \sigma(V^T x)$ forms a stochastic basis, and thus, the approximation property holds for all inputs, $x \in \Re^a$, in the compact set S [20]. Also, the functional approximation error is bounded such that $\|\varepsilon\| < \varepsilon_N$, where ε_N is a known bound and dependent on S [20]. The sigmoid activation function is considered here. For complete details of the NN and its properties, see [20].

Remark 1: Throughout this paper, $\|\cdot\|$ and $\|\cdot\|_F$ will be used interchangeably as the Frobenius vector and matrix norms, respectively [20].

B. Leader–Follower Tracking Control

To complete the separation–bearing formation control objective (1), contributions from single-robot control frameworks such as [23] are extended to leader–follower formation control. Consider the tracking controller error system from [23] for a single robot as

$$
e_j = T_{ej}(q_{jr} - q_j)
$$
$$
= \begin{bmatrix} e_{j1} \\ e_{j2} \\ e_{j3} \end{bmatrix} = \begin{bmatrix} \cos\theta_j & \sin\theta_j & 0 \\ -\sin\theta_j & \cos\theta_j & 0 \\ 0 & 0 & 1 \end{bmatrix} \begin{bmatrix} x_{jr} - x_j \\ y_{jr} - y_j \\ \theta_{jr} - \theta_j \end{bmatrix}
$$
$$
\dot{x}_{jr} = v_{jr}\cos\theta_{jr}, \qquad \dot{y}_{jr} = v_{jr}\sin\theta_{jr}
$$
$$
\dot{\theta}_{jr} = \omega_{jr}, \qquad \dot{q}_{jr} = \begin{bmatrix} \dot{x}_{jr} & \dot{y}_{jr} & \dot{\theta}_{jr} \end{bmatrix}^T \qquad (4)
$$

where x_{jr}, y_{jr}, θ_{jr}, and $\overline{v}_{jr} = \begin{bmatrix} v_{jr} & \omega_{jr} \end{bmatrix}^T$ are the Cartesian positions in the x- and y-directions, and the orientation and the linear and angular velocities, respectively, of a virtual reference robot for robot j [23]. In a single-robot control, a steering control input $v_{jc}(t)$ is designed to solve the following three basic problems: path following, point stabilization, and trajectory following such that $\lim_{t\to\infty}(q_{jr} - q_j) = 0$ and $\lim_{t\to\infty}(\overline{v}_{jr} - \overline{v}_j) = 0$ [23]. If the mobile robot controller can successfully track a class of smooth velocity control inputs, then all three problems can be solved with the same controller [23].

To extend the contributions from single-robot control frameworks such as (4) to leader–follower formation control, we begin by replacing the virtual reference cart with a physical mobile robot acting as the leader i for follower j subject to kinematics and dynamics that are defined similarly to (2) and (3), respectively. Then, define a reference position at a desired

separation L_{ijd} and a desired bearing Ψ_{ijd} for follower j with respect to the rear of leader i as

$$
x_{jr} = x_i - d_i\cos\theta_i + L_{ijd}\cos(\Psi_{ijd} + \theta_i)
$$
$$
y_{jr} = y_i - d_i\sin\theta_i + L_{ijd}\sin(\Psi_{ijd} + \theta_i) \qquad (5)
$$

as well as a reference orientation θ_{jr} that will be defined in the succeeding discussion. Next, define the actual position and orientation of follower j as

$$
x_j = x_i - d_i\cos\theta_i + L_{ij}\cos(\Psi_{ij} + \theta_i)
$$
$$
y_j = y_i - d_i\sin\theta_i + L_{ij}\sin(\Psi_{ij} + \theta_i)
$$
$$
\theta_j = \theta_j \qquad (6)
$$

where L_{ij} and Ψ_{ij} are the actual separation and bearing of follower j measured relative to the rear of the leader i. Substitution of (5) and (6) into the error system (4), and applying basic trigonometric identities, the kinematic error for leader–follower formation control is obtained as

$$
e_j = \begin{bmatrix} e_{j1} \\ e_{j2} \\ e_{j3} \end{bmatrix} = \begin{bmatrix} L_{ijd}\cos(\Psi_{ijd} + \theta_{ij}) - L_{ij}\cos(\Psi_{ij} + \theta_{ij}) \\ L_{ijd}\sin(\Psi_{ijd} + \theta_{ij}) - L_{ij}\sin(\Psi_{ij} + \theta_{ij}) \\ \theta_{jr} - \theta_j \end{bmatrix} \qquad (7)
$$

where $\theta_{ij} = \theta_i - \theta_j$ and θ_{jr} is the reference orientation. Due to the nonholonomic constraint as well as the separation–bearing formation control objective, the orientations of each robot in the formation will not be equal while the formation is turning, and thus, the reference orientation of each robot cannot be chosen such that $\theta_{jr} = \theta_i$. However, choosing the reference orientation relative to the leader satisfying the differential equation

$$
\dot{\theta}_{jr} = \frac{1}{d_j}\left(\omega_i L_{ijd}\cos(\psi_{ijd} + \theta_{ij}) + v_i\sin(\theta_{ijr}) + k_{j2}e_{j2}\right) \qquad (8)
$$

the asymptotic stability of all three error states can be shown, where $\theta_{ijr} = \theta_i - \theta_{jr} \in [-\pi, \pi]$ and k_{j2} is a positive design constant. Furthermore, it can be shown that the reference orientation of the follower will become equal to the orientation of the leader ($\theta_i - \theta_{jr} = 0$) after formation errors have converged to zero and when $v_i > 0$ and $\omega_i = 0$ which is a desirable attribute. The transformed error system (7) now acts as a formation tracking controller which not only seeks to remain at a fixed desired distance L_{ijd} with a desired angle Ψ_{ijd} relative to the leader robot i but will also achieve a relative orientation with respect to the leader. By taking the desired separation and bearing, L_{ijd} and Ψ_{ijd}, as constants similar to other works, and observing the derivatives of the separation and bearing, $\dot{L}_{ij}$ and $\dot{\Psi}_{ij}$ defined in [2], the error dynamics of (7) are found to be

$$
\begin{bmatrix} \dot{e}_{j1} \\ \dot{e}_{j2} \\ \dot{e}_{j3} \end{bmatrix} = \begin{bmatrix} -v_j + v_i\cos\theta_{ij} + \omega_j e_{j2} - \omega_i L_{ijd}\sin(\Psi_{ijd} + \theta_{ij}) \\ -\omega_j e_{j1} + v_i\sin\theta_{ij} - d_j\omega_j + \omega_i L_{ijd}\cos(\Psi_{ijd} + \theta_{ij}) \\ \frac{1}{d_j}(\omega_i L_{ijd}\cos(\Psi_{ijd} + \theta_{ij}) + v_i\sin(\theta_{ijr}) + k_{j2}e_{j2}) - \omega_j \end{bmatrix}. \qquad (9)
$$

To stabilize the kinematic system, we propose the velocity control inputs which are derived using Lyapunov methods for follower robot j to achieve the desired position and orientation

with respect to leader i as (10), shown at the bottom of the page, where $K_j = [k_{j1} \quad k_{j2} \quad k_{j3}]^T$ is a vector of positive design constants. Next, define the velocity tracking error as

$$e_{jc} = [e_{j4} \quad e_{j5}]^T = v_{jc} - \overline{v}_j = [v_{jc1} \quad v_{jc2}]^T - [v_j \quad \omega_j]^T. \tag{11}$$

Observing $\overline{v}_j = v_{jc} - e_{jc}$, substituting the control velocity (10) into the error dynamics of (9), and applying basic trigonometric identities reveal (12), shown at the bottom of the page. Examining the closed-loop error dynamics (12), it is clear that the stability of the kinematic system is dependent on the velocity tracking error. Additionally, the origin $e_j = 0$ and $e_{jc} = 0$ consisting of the position, orientation, and velocity tracking errors for follower j is an equilibrium point of the closed-loop kinematic error dynamics (12).

C. Dynamical NN/RISE Controller Design

In the previous section, it was shown that the stability of the kinematic error system depends on the velocity tracking error. Therefore, the dynamics of the mobile robot are now considered, and a velocity tracking loop is designed to ensure $\overline{v}_j \to v_{jc}$ asymptotically.

To begin the development, define the velocity filtered tracking errors as

$$r_j = \dot{e}_{jc} + \alpha_j(t)e_{jc} \tag{13}$$

where $\alpha_j(t)$ is a time-varying real function greater than zero that is defined as $\alpha_j(t) = \alpha_{j0} + \alpha_{j1}(t)$, where α_{j0} is a constant and $\alpha_{j1}(t)$ is a time-varying term. Multiplying both sides of (13) by $\overline{M}_j$, adding and subtracting $\overline{V}_{m_j}v_{jc}$ and $\overline{F}_j(v_{jc})$, and substituting the robot dynamics (3) allow (13) to be rewritten as

$$\overline{M}_j r_j = f_{d_j} + T_j + \overline{\tau}_{d_j} - \overline{\tau}_j \tag{14}$$

where

$$f_{d_j} = \overline{M}_j \dot{v}_{jc} + \overline{V}_{m_j} v_{jc} + \overline{F}_j(v_{jc})$$
$$T_j = e_{jc}\left(\alpha_j(t)\overline{M}_j - \overline{V}_{m_j}\right) + \overline{F}_j(\overline{v}_j) - \overline{F}_j(v_{jc}). \tag{15}$$

Differentiating (14) then yields the filtered tracking error dynamics

$$\overline{M}_j \dot{r}_j = -\dot{\overline{M}}_j r_j + \dot{f}_{d_j} + \dot{T}_j + \dot{\overline{\tau}}_{d_j} - \dot{\overline{\tau}}_j. \tag{16}$$

Using the *universal approximation property* for NNs [20], define $\dot{f}_{d_j} = W_j^T \sigma(V_j^T x_{dj}) + \varepsilon_j$, where W_j^T and V_j^T are the bounded constant ideal weights such that $\|W_j\|_F \leq W_M$ for a known constant W_M, ε_j is the bounded NN reconstruction error such that $\|\varepsilon_j\| \leq \varepsilon_{jM}$, $\|\dot{\varepsilon}_j\| \leq \varepsilon'_{jM}$ for known constants ε_{jM} and ε'_{jM}, and $x_{dj} = [1 \quad v_{jc} \quad \dot{v}_{jc} \quad \ddot{v}_{jc} \quad \theta_j]^T$. Examining the definition of the NN input x_{dj} reveals that $\dot{v}_{jc}$ and $\ddot{v}_{jc}$ are necessary; however, recalling v_{jc} in (10) that is a function of the leader's velocity reveals that $\dot{v}_{jc} = f_j(\dot{v}_i, \dot{\omega}_i, v_i, \omega_i, e_j, \dot{e}_j)$, where $f_j(\bullet)$ is the function describing $\dot{v}_{jc}$. The leader i's dynamics written in the form of (3) can be rewritten as $\dot{\overline{v}}_i = \overline{M}_i^{-1}(\overline{\tau}_i - \overline{F}_i(\overline{v}_i) - \overline{V}_{mi}\overline{v}_i)$, and substituting $\dot{\overline{v}}_i$ and (9) into $f_j(\bullet)$ results in the kinematic error dynamics of follower j and the dynamics of leader i to become a part of $\dot{v}_{jc}$ as

$$\dot{v}_{jc} = f_j(\overline{v}_i, \theta_i, \tau_i, \overline{v}_j, \theta_j, e_j). \tag{17}$$

It is not difficult to observe that $\dot{\overline{v}}_i$, v_{jc}, and $\dot{v}_{jc}$ are also smooth functions since the leader and follower robots' dynamics are sufficiently smooth. As a consequence, $\ddot{v}_{jc}$ can be approximated with relatively small error by the standard second-order backward difference equation for a small sample period Δt as

$$\ddot{v}_{jc} = v_{jc}(t) - 2v_{jc}(t - \Delta t) + v_{jc}(t - 2\Delta t). \tag{18}$$

Using (18) and forming $\dot{v}_{jc}$ under the assumption that $\dot{v}_i = 0$, as well as including the terms $\overline{v}_i$, θ_i, and τ_i of the function defined in (17), the estimated input to the NN $\hat{x}_{dj}$ takes the form of $\hat{x}_{dj} = [1 \quad v_{jc}^T \quad \dot{v}_{jc}^T|_{\dot{v}_i=0} \quad \ddot{v}_{jc}^T \quad \theta_j \quad \overline{v}_i \quad \tau_i^T \quad \theta_i \quad e_j^T]^T$ so that the dynamics of the leader i can be estimated by the NN, and the terms of $\dot{v}_{jc}$ omitted by assuming $\dot{v}_i = 0$ can be accounted for.

Remark 3: In the formation of the estimated NN input $\hat{x}_{dj}$, the terms $\overline{v}_i$, τ_i^T, and θ_i are considered available via a wireless communication link which is a standard assumption (see [13]).

The NN approximation of $\dot{f}_{d_j}$ is now defined as

$$\dot{\hat{f}}_{d_j} = \hat{W}_j^T \sigma\left(V_j^T \hat{x}_{dj}\right) \tag{19}$$

where $\hat{W}_j^T$ is the NN estimate of the ideal weight matrix W_j^T, and the control torque is now defined similarly [19] to be

$$\overline{\tau}_j = \hat{f}_{d_j} + \mu_j \tag{20}$$

$$v_{jc} = \begin{bmatrix} v_{jc1} \\ v_{jc2} \end{bmatrix} = \begin{bmatrix} v_i \cos\theta_{ij} + k_{j1}e_{j1} - \omega_i L_{ijd}\sin(\Psi_{ijd} + \theta_{ij}) \\ \frac{1}{d_j}\left(\omega_i L_{ijd}\cos(\Psi_{ijd} + \theta_{ij}) + v_i \sin(\theta_{ijr}) + k_{j2}e_{j2} + k_{j3}e_{j3}\right) \end{bmatrix} \tag{10}$$

$$\begin{bmatrix} \dot{e}_{j1} \\ \dot{e}_{j2} \\ \dot{e}_{j3} \end{bmatrix} = \begin{bmatrix} -k_{j1}e_{j1} + \omega_j e_{j2} + e_{j4} \\ 2v_i \sin\left(\frac{e_{j3}}{2}\right)\cos\left(\theta_i - \frac{\theta_{jr} + \theta_j}{2}\right) - k_{j2}e_{j2} - k_{j3}e_{j3} - \omega_j e_{j1} + d_j e_{j5} \\ -\frac{k_{j3}}{d_j}e_{j3} + e_{j5} \end{bmatrix} \tag{12}$$

where μ_j is the RISE feedback term defined similarly to [18] and [19] as

$$\mu_j = (k_{js}+1)e_{jc}(t) - (k_{js}+1)e_{jc}(0)$$
$$+ \int_0^t \left[(k_{js}+1)\alpha_j(s)e_{jc}(s) + (\beta_{j1}(s)+\beta_{j2})\mathrm{sgn}\,(e_{jc}(s)) \right] ds$$

(21)

such that $\dot{\mu}_j = (k_{js}+1)r_j + (\beta_{j1}(t)+\beta_{j2})\mathrm{sgn}(e_{jc})$, with $\beta_{j1}(t)$ being a real positive time-varying gain function, k_{js} and β_{j2} being positive real constants, and $\mathrm{sgn}(\bullet)$ being the signum function.

Remark 4: The projection algorithm is not used in this work to tune the NN weights as in [19], and as a result, the constant gains of [19] become time varying. Here, $\beta_{j1}(t)$ and $\alpha_j(t)$ are time-varying functions to facilitate in defining the upper bounds necessary for the RISE aspects of the NN/RISE controller which will be discussed in the succeeding development and in the Appendix in comparison to [18] and [19]. Furthermore, the constant term β_{j2} is not the same as the constant term β_2 from [18] and [19] and is included here to aid in the forthcoming stability analysis.

Next, substituting the derivative of (20), as well as adding and subtracting e_{jc} and $W_j^T \hat{\sigma}(V_j^T \hat{x}_{dj})$ into (16), yields

$$\overline{M}_j \dot{r}_j = -\frac{1}{2}\dot{\overline{M}}_j r_j + \widetilde{N}_j + N_{Bj1} + N_{Bj2}$$
$$- e_{jc} - (k_{js}+1)r_j - (\beta_{j1}(t)+\beta_{j2})\mathrm{sgn}(e_{jc}) \quad (22)$$

where

$$\widetilde{N}_j = -\frac{1}{2}\dot{\overline{M}}_j r_j + \dot{T}_j + e_{jc} \quad (23)$$
$$N_{Bj1} = \varepsilon_j + \dot{\overline{\tau}}_{d_j} + W_j^T \widetilde{\sigma}_j$$
$$N_{Bj2} = \widetilde{W}_j^T \sigma\left(V_j^T \hat{x}_{dj}\right) = \widetilde{W}_j^T \hat{\sigma}_j \quad (24)$$

and $\widetilde{W}_j = W_j - \hat{W}_j$, $\widetilde{\sigma}_j = \sigma(V_j^T x_{dj}) - \sigma(V_j^T \hat{x}_{dj})$. An upper bound for $\widetilde{N}_j$ can be obtained using the mean value theorem as [18] and [19]

$$\|\widetilde{N}_j\| \le \rho\left(\|z_j\|\right)\|z_j\| \quad (25)$$

where $z_j = [e_{jc}^T \quad r_j^T]^T$ and $\rho(\|z_j\|)$ is a positive globally invertible nondecreasing function.

Lemma 1: The expressions in (24) and their derivatives are upper bounded according to

$$\|N_{Bj1}\| \le \varepsilon_N + d'_M + 2W_M\sqrt{N_h}$$
$$\equiv \varsigma_{j1} \quad (26)$$
$$\|\dot{N}_{Bj1}\| \le \varepsilon'_N + d'_M + (\sqrt{N_h} + N_h)(C_1 + C_2\|e_j\|)$$
$$\equiv \varsigma'_{j1}(t) \quad (27)$$
$$\|N_{Bj2}\| \le \left(W_M + \|\hat{W}_j\|_F\right)\sqrt{N_h}$$
$$\equiv \varsigma_{j2}(t) \quad (28)$$

$$\|\dot{N}_{Bj2}\| \le C_3\|e_{jc}\| + (\sqrt{N_h} + N_h)\left(W_M + \|\hat{W}_j\|_F\right)c_2(t)$$
$$\equiv \varsigma'_{j2}(t) \quad (29)$$

where C_1, C_2, and C_3 are known positive constants and $c_2(t)$ is a positive time-varying function based on $\|\dot{\hat{x}}_{dj}\|$.

Proof: See the Appendix.

To aid in the forthcoming stability analysis and to facilitate time-varying gains, we define an auxiliary function as $L_j = r_j^T(N_{Bj1} + N_{Bj2} - \beta_{j1}\mathrm{sgn}(e_{jc})) - e_{jc}^T N_{Bj2} - \dot{\beta}_{j1}\|e_{jc}\| - \dot{e}_{jc}^T \beta_{j2}\mathrm{sgn}(e_{jc}) - \alpha_{jo}\beta_{j2}\|e_{jc}\|$.

Lemma 2: Given the auxiliary function L_j, let $\beta_{j1}(t)$ and β_{j2} be chosen according to

$$\beta_{j1}(t) \ge K_{j\beta} + K_{jW}\|\hat{W}_j\|_F$$
$$+ K_{je}\|e_j\| + K_{jWe}\|e_j\|\,\|\hat{W}_j\|_F + K_{jec}\|e_{jc}\|$$
$$\beta_{j2} > 0 \quad (30)$$

with $K_{j\beta}$, K_{jW}, K_{je}, K_{jWe}, and K_{jec} being known positive constants, and then

$$\int_0^t L_j(s)ds \le \gamma_j$$

where $\gamma_j = \|e_{jc}(0)\|(\beta_{j1}(0)+\beta_{j2}) - e_{jc}^T(0)N_{Bj3}(0) \ge 0$, with $N_{Bj3} = N_{Bj1} + N_{Bj2}$.

Proof: See the Appendix.

Before proceeding, it is important to note that $r_j = 0$, $e_{jc} = 0$, and $\widetilde{W}_j^T = 0$ are the equilibrium points of (22) in the absence of disturbances and NN functional reconstruction error $(N_{Bj1} = 0)$. The proof of this claim is straightforward through the examination of (13) and (22).

Theorem 1—(Follower Dynamic Control): Given the nonholonomic robot system consisting of (2) and (3) along with the leader follower criterion of (1), let a smooth velocity control input $v_{jc}(t)$ for follower j be given by (10), and let the torque control for follower j given by (20) be applied to (3). Let the NN weight tuning law be given as

$$\dot{\hat{W}}_j = F_j \hat{\sigma}_j e_{jc}^T \quad (31)$$

where $F_j = F_j^T > 0$ is a design parameter. Then, there exists a vector of positive constants $K_j = [k_{j1} \quad k_{j2} \quad k_{j3}]^T$, positive constants k_{js}, β_{j2}, and α_{j0}, and positive time-varying functions $\beta_{j1}(t)$ and $\alpha_j(t)$, such that the position, orientation, and velocity tracking errors e_j and e_{jc} are AS, and the NN weight estimate errors $\widetilde{W}_j$ are bounded for follower j, provided that $\beta_{j1}(t)$ and β_{j2} are selected as in (30).

Proof: See the Appendix.

D. Leader Control Structure

In every formation, there is a formation leader i whose kinematics and dynamics are defined similarly to (2) and (3), respectively. From [23], the leader tracks a virtual reference

robot, and the tracking error for the leader and its derivative are found to be

$$e_i = \begin{bmatrix} e_{i1} \\ e_{i2} \\ e_{i3} \end{bmatrix} = \begin{bmatrix} \cos\theta_i & \sin\theta_i & 0 \\ -\sin\theta_i & \cos\theta_i & 0 \\ 0 & 0 & 1 \end{bmatrix} \begin{bmatrix} x_r - x_i \\ y_r - y_i \\ \theta_r - \theta_i \end{bmatrix}$$

$$\dot{e}_i = \begin{bmatrix} \dot{e}_{i1} \\ \dot{e}_{i2} \\ \dot{e}_{i3} \end{bmatrix} = \begin{bmatrix} -v_i + v_{ir}\cos e_{i3} + \omega_i e_{i2} \\ -\omega_i e_{i1} + v_{ir}\sin e_{i3} \\ \omega_{ir} - \omega_i \end{bmatrix} \quad (32)$$

where x_{ir}, y_{ir}, θ_{ir}, v_{ir}, and ω_{ir} are the states of a virtual reference robot for leader i defined as in (4). In this work, the virtual leader's velocity $\overline{v}_{ir} = [v_{ir} \quad \omega_{ir}]^T$ is defined by a time-varying function that is twice differentiable. The leader's control velocity $v_{ic}(t)$ is then defined similarly to [23] as

$$v_{ic} = \begin{bmatrix} v_{ic1} \\ v_{ic2} \end{bmatrix} = \begin{bmatrix} v_{ir}\cos e_{i3} + k_{i1}e_{i1} \\ \omega_{ir} + k_{i2}v_{ir}e_{i2} + k_{i3}k_{i2}\sin e_{i3} \end{bmatrix} \quad (33)$$

where $K_i = [k_{i1} \quad k_{i2} \quad k_{i3}]^T$ is a vector of positive constants, and the third term of v_{ic2} in (33) has been altered from [23] to facilitate in the stability analysis to come. To construct the dynamical NN/RISE controller for the leader i, define the velocity tracking and filtered tracking errors as

$$e_{ic} = v_{ic} - \overline{v}_i \qquad r_i = \dot{e}_{ic} + \alpha_i(t)e_{ic}. \quad (34)$$

Using similar steps and justifications that are used to form (14) for follower j, construct the error system for leader i to be $\overline{M}_i r_i = f_{d_i} + T_i + \overline{\tau}_{d_i} - \overline{\tau}_i$, where f_{d_i} and T_i are defined similarly to (15). The control torque $\overline{\tau}_i$ for leader i can be defined similarly to follower j's as

$$\overline{\tau}_i = \hat{f}_{d_i} + \mu_i \quad (35)$$

where $\hat{f}_{d_i}$ is the estimate of f_{d_i}, μ_i is the RISE feedback term defined similarly to the follower's in (19)–(21). The NN input vector for leader i is defined as $\hat{x}_{di} = [1 \quad v_{ic}^T \quad \dot{v}_{ic}^T \quad \ddot{v}_{ic}^T|_{\dot{v}_i=0} \quad \theta_i \quad \overline{v}_i^T]^T$, where the term $\dot{v}_{ic}^T$ is available, while the term $\ddot{v}_{ic}^T$ is not due to its dependence on $\dot{\overline{v}}_i$ which is not known. As a result $\ddot{v}_{ic}^T$ is calculated assuming $\dot{\overline{v}}_i = 0$ and including the terms $\overline{v}_i$ and θ_i in $\hat{x}_{di}$ so that the unknown dynamics can be accounted for by the NN similarly to the treatment of (17).

Using the same steps and justifications that are used to form (22), the closed-loop error system for the lead robot i can be formed as

$$\overline{M}_i \dot{r}_i = -\frac{1}{2}\dot{\overline{M}}_i r_i + \widetilde{N}_i + N_{Bi1} + N_{Bi2} - e_{ic}$$
$$- (k_{is} + 1)r_i - (\beta_{i1}(t) + \beta_{i2})\,\mathrm{sgn}(e_{ic}) \quad (36)$$

where k_{is} is a positive control gain parameter, and $\widetilde{N}_i$, N_{Bi1}, and N_{Bi2} are defined similarly to (23) and (24), respectively, and are bounded similarly to the bounds defined in (25)–(29). Furthermore, $r_i = 0$, $e_{ic} = 0$, and $\widetilde{W}_i^T = 0$ are the equilibrium

points of (36) in the absence of disturbances and NN functional reconstruction error ($N_{Bi1} = 0$).

Theorem 2—(Leader Stability): Let the smooth velocity control input for leader i be given by (33), and let the toque control input defined by (35) be applied to the leader robot i, defined similarly to (3). Let the NN tuning law for leader i be defined similarly to (31). Then, there exist a vector of positive constants $K_i = [k_{i1} \quad k_{i2} \quad k_{i3}]^T$, positive constants k_{is}, β_{i2}, and α_{i0}, and positive time-varying functions $\beta_{i1}(t)$ and $\alpha_i(t)$, such that the position, orientation, and velocity tracking errors e_i and e_{ic} are AS, and the NN weight estimate errors $\widetilde{W}_i$ are bounded for follower j, provided that $\beta_{i1}(t)$ and β_{i2} are selected similarly to (30).

Proof: See the Appendix.

Next, the stability of the entire formation is demonstrated in the following theorem.

E. Formation Stability

Theorem 3—(Formation Stability): Consider a formation of $N + 1$ robots consisting a leader i and N followers, and let the hypotheses of *Theorems 1* and *2* hold. Then, the formation error $e_{ij} = [e_i^T \quad e_{ic}^T \quad e_j^T|_{j=1} \ldots, e_j^T|_{j=N} \quad e_{jc}^T|_{j=1} \ldots, e_{jc}^T|_{j=N}]^T$, where $e_{ij} \in \Re^{(n+\rho)(1+N)}$ represents the augmented position, orientation, and velocity tracking error systems for the leader i and N followers, respectively, is AS, and the NN weight estimation errors $\widetilde{W}_i^T$ and $\widetilde{W}_j^T$, $j = 1, 2, \ldots, N$, for the leader i and N followers, respectively, are bounded.

Proof: See the Appendix.

Remark 5: The stability of the entire formation for the case when follower j becomes a leader to follower $j + 1$ follows directly from *Theorem 1* and selecting a Lyapunov candidate to be the sum of the Lyapunov candidates for follower j and follower $j + 1$, respectively. In this case, follower j becomes the reference for follower $j + 1$, and thus, the dynamics of follower j must be considered by follower $j + 1$. Since the dynamics of follower j incorporates the dynamics of leader i, follower $j + 1$ inherently brings in the dynamics of leader i by considering the dynamics of follower j.

A general formation controller structure is shown in Fig. 2, which includes the controller structures for the leader i and multiple followers. Additionally, communication between the robots is indicated. In the figure, leader i communicates its velocity, orientation, and control torque to follower j, and follower j communicates its velocity, orientation, and control torque to follower $j + 2$, but it is not necessary for follower j to relay the states of leader i to follower $j + 2$. Also note that in a formation of robots, each robot may have more than one follower.

III. LEADER–FOLLOWER OBSTACLE AVOIDANCE

Next, a simple but effective obstacle avoidance scheme is proposed that will allow follower j to track its leader while simultaneously avoiding obstacles. To accomplish this, the desired separation and bearing are no longer considered to be constants but are considered to be time varying, and through the incorporation of RISE feedback, each follower in
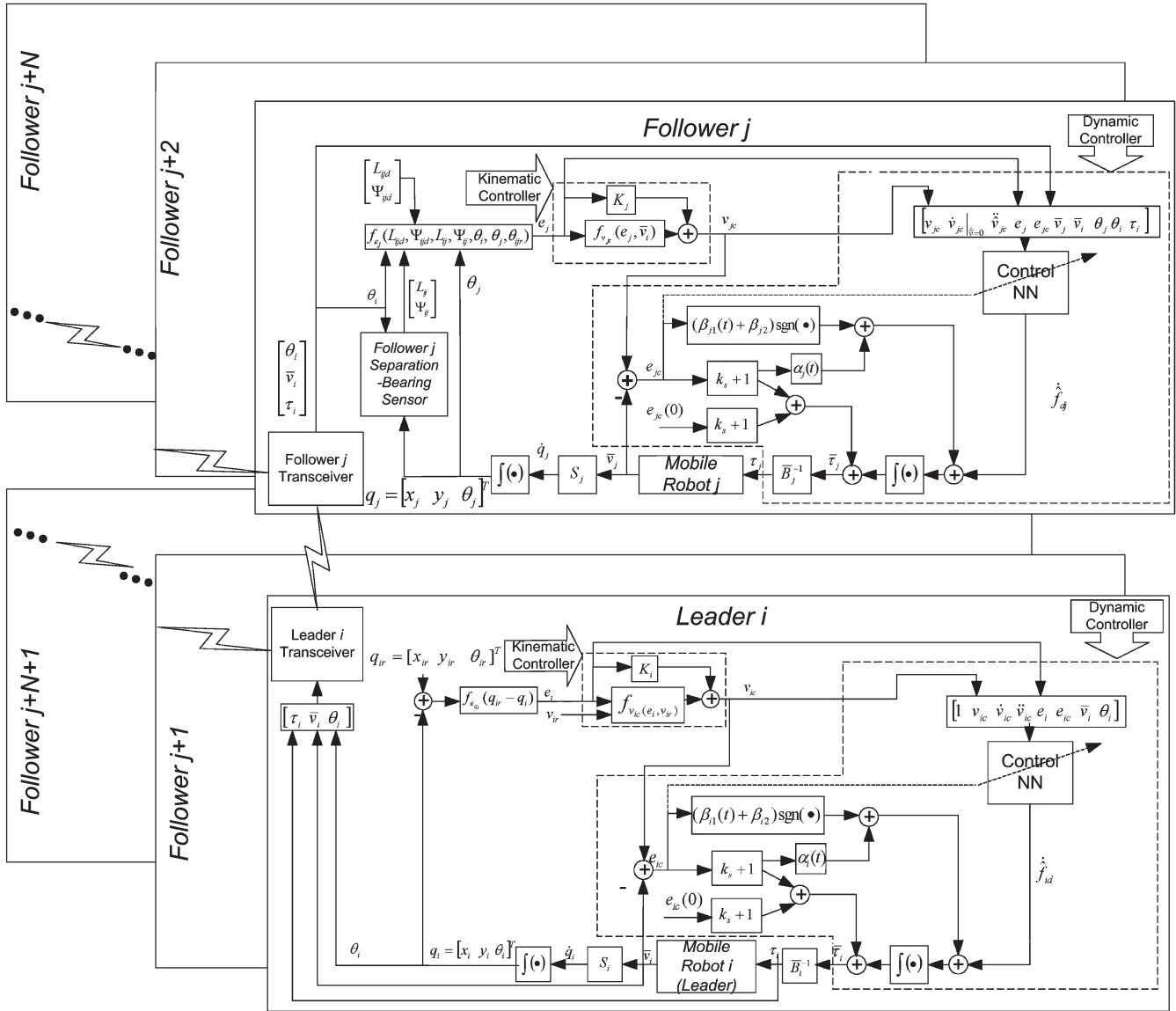
Fig. 2. General formation controller structure.

the formation asymptotically tracks the new reference position while avoiding obstacles. In this section, the time-varying desired separation and bearing will be denoted as $L_{ijd}(t)$ and $\Psi_{ijd}(t)$, while the constant desired separation and bearing will be written as L_{ijd} and Ψ_{ijd}, respectively. Furthermore, the distance from the center of follower j to an obstacle s_j and the relative angle of the obstacle θ_{js} are considered measurable, while the velocity vector $\overline{v}_o = [v_o \quad \omega_o]^{\mathrm{T}}$ and orientation θ_o of the obstacle are unavailable. It is standard to assume that the formation leader i utilizes a path planning scheme such that, by tracking the virtual reference cart described in [23], the lead robot i navigates around any encountered obstacles.

To begin with, consider the configuration shown in Fig. 3, where it is desirable that the follower robot j maintains a safe distance s_d from the closest obstacle. When the nearest edge of an obstacle is detected at angle θ_{js} and distance s_j relative to the center of follower j such that $s_j < s_d$, the desired separation and bearing, $L_{ijd}(t)$ and $\Psi_{ijd}(t)$, respectively, are

modified to ensure that the follower is steered away from the obstacle by

$$L_{ijd}(t) = L_{ijd} - \frac{1}{2} K_L \left(\frac{1}{s_j} - \frac{1}{s_d} \right)^2 \mathrm{sgn}(\theta_{js}\Psi_{ijd})$$

$$\Psi_{ijd}(t) = \Psi_{ijd} + \frac{1}{2} K_\Psi \left(\frac{1}{s_j} - \frac{1}{s_d} \right)^2 \xi_j \qquad (37)$$

where $\xi_j = \mathrm{sgn}(\Psi_{ijd})\mathrm{sgn}(\theta_{js}\Psi_{ijd})$, with sgn being the signum function and K_L and K_ψ being positive design constants. Examining (37), one can see that the shifts introduced to the desired separation and bearing are similar to repulsive potential functions commonly used in robotic path planning [22]. Here, we use the potential-like function to push the desired set point of the follower robot j away from the encountered obstacle, thus steering the robot around the obstruction. Incorporation of $\mathrm{sgn}(\theta_{js}\Psi_{ijd})$ allows obstacles to be avoided on the left or the right, depending on where the follower is located in the formation and where the obstacle is located relative to the
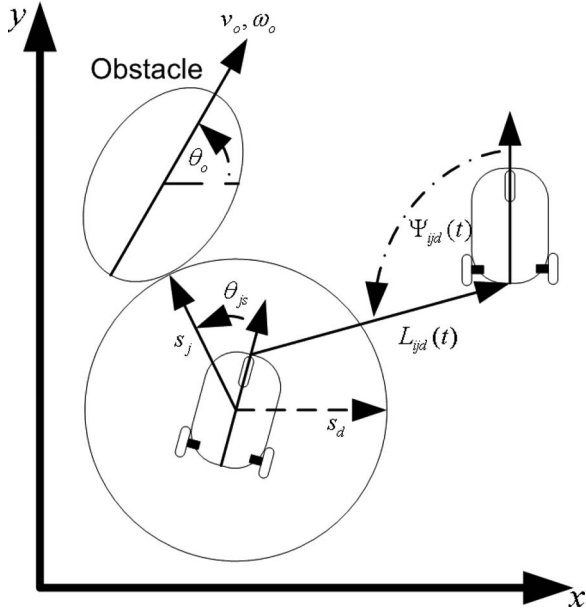
Fig. 3. Obstacle avoidance.

follower. This term also allows collisions to be avoided within the formation by considered neighboring robots as obstacles.

With the introduction of obstacle avoidance schemes, the orientation of the follower j will vary from its reference orientation as a result of avoiding an obstacle that was in the path of the follower j but not its leader. Therefore, while avoiding an obstacle, it is logical for follower j to track a reference point, but no specific orientation with respect to its leader. Thus, consider the formation tracking control error system presented in (7), but it is rewritten to include only the normal and tangential position error components as

$$e_{jo} = \begin{bmatrix} e_{jo1} \\ e_{jo2} \end{bmatrix}$$
$$= \begin{bmatrix} L_{ijd}(t) \cos\left(\Psi_{ijd}(t)+\theta_{ij}\right) - L_{ij}\cos\left(\Psi_{ij}+\theta_{ij}\right) \\ L_{ijd}(t) \sin\left(\Psi_{ijd}(t)+\theta_{ij}\right) - L_{ij}\sin\left(\Psi_{ij}+\theta_{ij}\right) \end{bmatrix}. \quad (38)$$

The dynamics of (38) can be found in a similar manner as that of (9) and is written as (39), shown at the bottom of the page, where

$$\dot{\bar{e}}_{jo1} = \dot{L}_{ijd}(t) \cos\left(\Psi_{ijd}(t) + \theta_{ij}\right) \\ - \dot{\Psi}_{ijd}(t) L_{ijd}(t) \sin\left(\Psi_{ijd}(t) + \theta_{ij}\right)$$

$$\dot{\bar{e}}_{jo2} = \dot{L}_{ijd}(t) \sin\left(\Psi_{ijd}(t) + \theta_{ij}\right) \\ + \dot{\Psi}_{ijd}(t) L_{ijd}(t) \cos\left(\Psi_{ijd}(t) + \theta_{ij}\right). \quad (40)$$

The dynamics of the desired separation and bearing, $L_{ijd}(t)$ and $\Psi_{ijd}(t)$ in (37), respectively, are necessary in the calculation of (40), and therefore, the derivative $\dot{s}_j$ is also required. The measured distance s_j can be written in terms of the x and y components of s_j as $s_j^2 = s_{jx}^2 + s_{jy}^2$, where $s_{jx} = x_j - x_o$ and $s_{jy} = y_j - y_o$, with x_o and y_o being the coordinates of the obstacle. Note that the obstacle is not necessarily stationary, and therefore, assume that the obstacle can be described using the kinematic model as $\dot{x}_o = v_o \cos\theta_o$ and $\dot{y}_o = v_o \sin\theta_o$. Using this information along with (2), it is evident that the derivative of s_j is a function of the velocity $\bar{v}_j$ and orientation θ_j of follower j as well as the velocity $\bar{v}_o$ and orientation θ_o of the encountered obstacle. Since the velocity $\bar{v}_o$ and orientation θ_o of the obstacle are not available to follower j, $\dot{s}_j$ must be estimated, and as a result, $\dot{L}_{ijd}(t)$ and $\dot{\Psi}_{ijd}(t)$ must also be estimated. Assuming that s_j is a smooth function, define the aforementioned estimates to be

$$\dot{\hat{L}}_{ijd}(t) = \operatorname{sgn}(\theta_{js}\Psi_{ijd})K_L \left(\frac{1}{s_j} - \frac{1}{s_d}\right) \frac{1}{s_j^2}\dot{\hat{s}}_j$$
$$\dot{\hat{\Psi}}_{ijd}(t) = -\xi_j K_\psi \left(\frac{1}{s_j} - \frac{1}{s_d}\right) \frac{1}{s_j^2}\dot{\hat{s}}_j \quad (41)$$

and $\dot{\hat{s}}_j = s_j(t) - s_j(t - \Delta t)$ is the estimate of $\dot{s}_j$ for an arbitrarily small time interval Δt.

In order to show that the obstacle avoidance method is AS in the presence of uncertainties, the RISE method described in the previous section will again be utilized. To use the RISE method, we begin by defining a filtered tracking error as

$$\vartheta_j = \dot{e}_{jo} + \kappa e_{jo} \quad (42)$$

where κ is a positive real design constant. Utilizing the error dynamics (39) and (40), the filtered tracking error (42) can be rewritten as

$$\vartheta_j = J_j + H_j - E_j v_j + \kappa e_{jo} \quad (43)$$

where J_j, H_j, and Ej are defined in (44) and (45), shown at the bottom of the page, and $\dot{s}_j$ is the real dynamics of s_j. To stabilize the filtered tracking error dynamics in the presence of

$$\begin{bmatrix} \dot{e}_{jo1} \\ \dot{e}_{jo2} \end{bmatrix} = \begin{bmatrix} \dot{\bar{e}}_{jo1} - v_j + v_i \cos\theta_{ij} + \omega_j e_{jo2} - \omega_i L_{ijd}(t) \sin\left(\Psi_{ijd}(t) + \theta_{ij}\right) \\ \dot{\bar{e}}_{jo2} - \omega_j e_{jo1} + v_i \sin\theta_{ij} - d_j \omega_j + \omega_i L_{ijd}(t) \cos\left(\Psi_{ijd}(t) + \theta_{ij}\right) \end{bmatrix} \quad (39)$$

$$J_j = \left(\frac{1}{s_j} - \frac{1}{s_d}\right)\frac{1}{s_j^2}\dot{s}_j \begin{bmatrix} \operatorname{sgn}(\theta_{js}\Psi_{ijd})K_L \cos\left(\Psi_{ijd}(t)+\theta_{ij}\right) + \xi_j K_\Psi L_{ijd}(t) \sin\left(\Psi_{ijd}(t)+\theta_{ij}\right) \\ \operatorname{sgn}(\theta_{js}\Psi_{ijd})K_L \sin\left(\Psi_{ijd}(t)+\theta_{ij}\right) - \xi_j K_\Psi L_{ijd}(t) \cos\left(\Psi_{ijd}(t)+\theta_{ij}\right) \end{bmatrix} \quad (44)$$

$$H_j = \begin{bmatrix} v_i \cos(\theta_{ij}) - \omega_i L_{ijd}(t) \sin\left(\Psi_{ijd}(t)+\theta_{ij}\right) + e_{jo2}\omega_j \\ v_i \sin(\theta_{ij}) + \omega_i L_{ijd}(t) \cos\left(\Psi_{ijd}(t)+\theta_{ij}\right) - e_{jo1}\omega_j \end{bmatrix} \qquad E_j = \begin{bmatrix} 1 & 0 \\ 0 & d_j \end{bmatrix} \quad (45)$$

an obstacle, the following velocity control input for follower robot j is proposed:

$$v_{jco} = E_j^{-1}\left(H_j + \hat{J}_j + (G + \kappa)e_{jo} \right.$$
$$\left. + \int_0^t (G\kappa e_{jo} + \beta_{jo}\mathrm{sgn}(e_{jo}))\,ds \right) \in \Re^2 \quad (46)$$

where $\hat{J}_j$ is the estimate of J_j as a result of using $\dot{\hat{s}}_j$, and G and β_{jo} are positive real design constants. For analysis purposes, we will assume that $J_j = \hat{J}_j + \zeta_j$, where ζ_j is the error in estimation. Furthermore, we assume that the estimation error and its derivative are bounded by positive real values ζ_M and ζ_M', respectively, such that $\|\zeta_j\| \le \zeta_M$ and $\|\zeta_j'\| \le \zeta_M'$ for all time.

Defining the velocity tracking error e_{jco} identically to (11), substituting $\overline{v}_j = v_{jco} - e_{jco}$ into (43), and taking the derivative, the closed-loop kinematic filtered error dynamics can be written as

$$\dot{\vartheta}_j = -G\vartheta_j + \zeta_j - \beta_{jo}\mathrm{sgn}(e_{jo}) + E_j e_{jco} \quad (47)$$

and when there is zero estimation error, $\zeta_j = 0$, the origin $\vartheta_j = 0$, $e_{jo} = 0$, and $e_{jco} = 0$ is an equilibrium point of $\dot{\vartheta}_j$. To aid in the stability analysis of the follower robot in the presence of obstacles, an auxiliary function is defined as $R_j(t) = \vartheta_j^T(\zeta_j - \beta_{jo}\mathrm{sgn}(e_{jo}))$.

Lemma 3: Given the auxiliary function $R_j(t)$, then $\int_0^t R_j(s)\mathrm{d}s \le \beta_{jo}\|e_{jo}(0)\| - e_{jo}^T(0)\zeta_j(0)$, provided that β_{jo} is selected as

$$\beta_{jo} \ge \zeta_M + \frac{1}{\kappa}\zeta_M'. \quad (48)$$

Proof: See the Appendix.

Theorem 4—(Follower Obstacle Avoidance): Let the hypothesis of *Theorem 1* hold with (10) replaced by (46). Then, there exist positive constants G, β_{jo}, K_L, and K_ψ such that position and velocity tracking errors for the follower are AS in the presence of obstacles, provided that β_{jo} is selected as (48).

Proof: See the Appendix.

Remark 6: Since leader robot i does not track a physical robot, any existing AS obstacle avoidance method can be utilized by the leader to ensure the stability of the entire formation in the presence of obstacles. The path planning algorithm for the leader i is beyond the scope of this paper and is therefore not included here.

Remark 7: The stability of a formation of $N + 1$ robots consisting of a leader i and N followers in the presence of obstacles follows directly by combining the results of *Theorems 2* and *4* for $j = 1, 2, 3, \ldots, N$, respectively. Furthermore, the stability of a formation in the presence of obstacles for the case when follower j becomes a leader to follower $j + 1$ follows directly from *Theorem 4* and combining the Lyapunov candidates for follower j and follower $j + 1$ into a single Lyapunov function.

Remark 8: The proposed obstacle avoidance scheme is observed to have potential limitations. Since the scheme only

TABLE I
FRICTION COEFFICIENTS

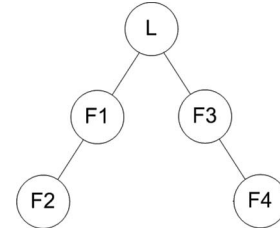|	L	F1	F2	F3	F4
μ_1	0.5	0.05	0.01	0.015	0.025
μ_2	0.75	0.75	0.65	0.15	0.50
μ_3	0.25	0.025	0.025	0.05	0.015
μ_4	0.03	0.30	0.20	0.25	0.03

Fig. 4. Formation structure.

considers the closest obstruction, it is possible that, in a highly cluttered environment, there may be more than one obstacle within the robot's safety zone; one of which could potentially be another robot in the formation. In this case, the follower may exhibit an oscillatory behavior between multiple obstructions located within the safety zone which is not ideal; however, the goal of the obstacle avoidance scheme is still achieved in that collisions are avoided. In the event that two or more obstacles are located at the same distance from follower j, the obstacle which poses the greatest immediate threat of collision is considered. Future efforts will work to remove these limitations, and the obstacle avoidance is not the focus of this effort.

Remark 9: The control velocity (46) can be applied for *any* obstacle avoidance scheme in which the desired separation and bearing are modified to steer the robot around the obstruction. The only required modification to the control velocity (46) is with respect to the vector J_j in (44) which contains the dynamics of $L_{ijd}(t)$ and $\Psi_{ijd}(t)$, respectively.

Remark 10: By the design of the obstacle avoidance scheme, the follower robot continues to track its leader while it navigates around an obstacle through the use of the time-varying desired separation and bearing. As the robot navigates around the obstruction and the obstruction leaves the robot's safety zone, the time-varying desired separation and bearing naturally return to the constant desired values. Thus, the robot itself returns to its location in the formation.

IV. SIMULATION RESULTS

A formation of identical nonholonomic mobile robots is considered, where the leader's trajectory is the desired formation trajectory, and simulations are carried out in MATLAB under the following two scenarios: with and without obstacles. In the first scenario, the NN controller which renders UUB in [15] is considered, and then, the NN/RISE controller which has been shown to be AS in this paper is tested. The torque controller developed in [15] is similar to the one in (20) but without the extra RISE terms added in (21) and takes the form of $\hat{\tau}_j = \hat{W}_j^T \sigma(\overline{x}_j) + (k_{js} + 1)e_{jc} = \hat{f}_j + (k_{js} + 1)e_{jc}$, where $\hat{f}_j$ is the NN estimate of an unknown function.
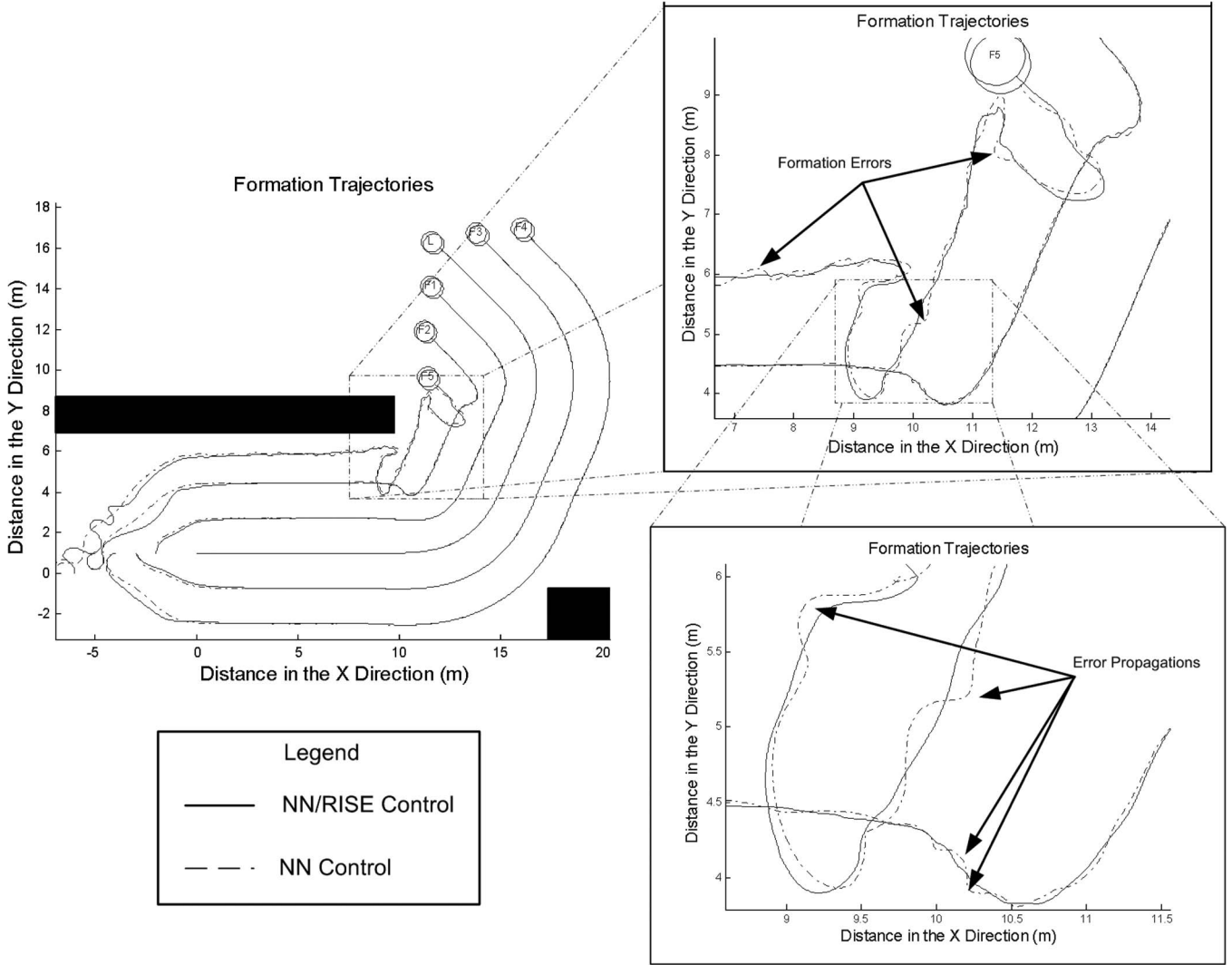
Fig. 5. Formation trajectories.

An additional difference between the torque control of this paper and that of [15] is the fact that the NN estimates the derivative of an unknown function in this work. In both cases, unmodeled dynamics are introduced in the form of friction as $\overline{F}_j = [\mu_{j1}\text{sign}(v_j) + \mu_{j2}v_j, \ \mu_{j3}\text{sign}(\omega_j) + \mu_{j4}\omega_j]^T$, where μ_{ji} denotes the coefficients of friction and summarized in Table I. Additionally, disturbance and sensor noise terms are added to the robot dynamics and state measurements, respectively. Disturbances are added to the robot dynamics and are generated from a normal distribution with mean zero, variance one, and standard deviation one. The magnitude of the disturbances is taken as two.

Sensor noise is also generated from an identical normal distribution with magnitudes of $\eta_v = 0.25$, $\eta_L = 0.1$, and $\eta_\Psi = 0.05$, where η_v, η_L, and η_Ψ are for the velocity, separation, and bearing measurements, respectively. In the second scenario, obstacles are added in the path of the follower robots, and the obstacle avoidance scheme of *Theorem 4* is demonstrated, and both static and dynamic obstacle environments are considered.

In the simulations, followers 1 and 2 track the leader, while followers 3 and 4 track followers 1 and 2, respectively, as shown in Fig. 4. The following parameters are considered for the leader and its followers: $m = 5$ kg, $I = 3$ kg^2, $R = 0.175$ m, $r = 0.08$ m, and $d = 0.4$ m. The control gains for the leader were selected as $k_{i1} = 10$, $k_{i2} = 5$, $k_{i3} = 4$, and $K_{is} = 35$, and for each follower, the gains were selected as $k_{j1} = 5$, $k_{j2} = 5$, $k_{j3} = 16.5$, and $K_{js} = 35$. Five hidden layer neurons are considered in the NN for the leader and each follower such that $N_h = 5$, and the NN parameters for both the leader and each follower were selected as $F_j = F_i = 10$. In addition, the RISE terms are selected according to (30), with $K_W = 8$, $K_e = 15$, $K_{We} = 8$, $K_\beta = 15$, and $K_{ec} = 10$, and the filtered tracking error gain $\alpha(t)$ is selected as $\alpha(t) = 5 + (1/\beta_2)(K_W\sqrt{N_h}F\|e_c\| + K_{ec}(10 + 2.5\|e\|) + K_e(8 + 2.5\|e\|) + K_{We}((8 + 2.5\|e\|) \times \|\hat{W}\|_F + F\sqrt{N_h}\|e_c\|\|e\|))$, with $\beta_2 = 20$.

Remark 11: In the succeeding analysis, L, $F1$, $F2$, $F3$, and $F4$ will be used to denote the *leader*, *follower 1*, *follower 2*, *follower 3*, and *follower 4*, respectively.

A. Scenario I: Obstacle-Free Environment

In this scenario, the leader follows a virtual robot traveling at a constant linear velocity of $v_{ir} = 5$ m/s with a time-varying
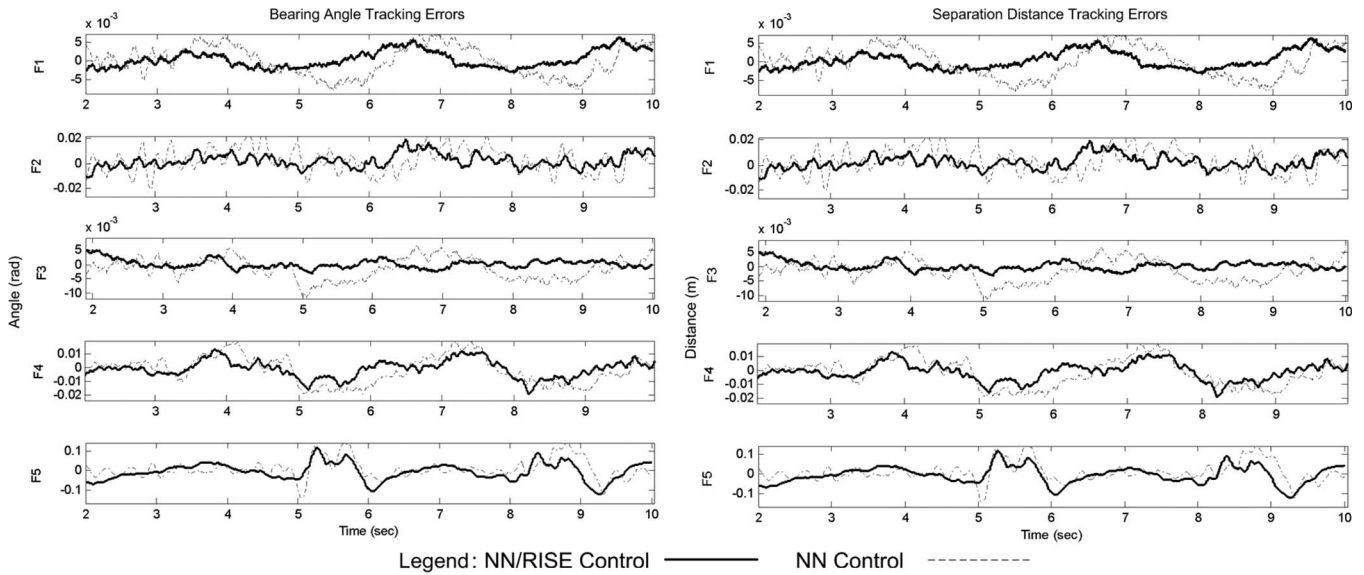
Fig. 6.   Formation errors.

TABLE II
AVERAGE STEADY-STATE FORMATION ERRORS

Average Errors	NN/RISE Controller					NN Controller				
	F1	F2	F3	F4	F5	F1	F2	F3	F4	F5
Separation error (m)	0.0048	0.0117	0.0029	0.0066	0.0442	0.0094	0.0179	0.0048	0.077	0.0462
Bearing error (rad)	0.0030	0.0069	0.0037	0.0049	0.0449	0.0036	0.0089	0.0041	0.0093	0.0467

reference angular velocity, and the NN controller of our previous work and the NN/RISE controller are tested. The formation is selected to be a wedge shape as in Fig. 4, where each follower is to track its leader at a desired separation of $L_{ijd} = 2$ m with a bearing of $\Psi_{ijd} = \pm 120°$, depending on the follower's location, and for illustrative purposes, a fifth follower has been added to track follower 2.

Fig. 5 shows the formation trajectories for both controllers as the formation performs a sharp turn while navigating around a barrier. Examining the trajectories reveals that both controllers successfully perform the maneuver; however, upon closer examination, formation errors are seen propagating throughout the formation for the case when the NN controller is used. The evidence of the error propagation is best seen in the trajectories of the robots on the inside of the turn, which have been enlarged to facilitate viewing. Examining the trajectories in the bottom right corner of Fig. 5, small errors can been seen in the path of follower 2, while larger errors are seen in the path of follower 5 for the case when the NN controller is applied. On the other hand, evidence of this error propagation is not present in the paths of either robot when the NN/RISE controller is applied. Thus, the theoretical conjectures of *Theorem 1* are verified in that the formation achieves asymptotic tracking in the presence of bounded disturbances.

Fig. 6 shows the steady-state formation errors of each follower in the formation. The improved performance of the NN/RISE controller over the NN controller is again observed, particularly in the formation errors for followers 1, 2, and 3, respectively, and the strength of AS over UUB is revealed. The average formation errors for each follower are shown in Table II, where it is observed that the average error was reduced

for each follower when the NN/RISE controller was utilized. In some cases, as with follower 1, errors were reduced by 50%, while marginal error reduction was observed for follower 5. Reducing the formation errors for the robots near the front of the formation helps prevent formation errors from propagating through the formation, which was observed for the case when the NN controller was applied.

Remark 12: The reference position of each robot in the formation is defined with respect to its respective leader, not the leader of the entire formation. As a result, the movement of each robot propagates to its followers, a phenomenon observed in Fig. 5 with followers 2 and 5 for the case when the NN control was applied. Additionally, it was observed in Table II that formation errors for follower 5 were marginally reduced when the NN/RISE controller was applied; however, although the reduction in the error was small, the improved performance in the NN/RISE controller over the standard NN controller is still significant since the oscillatory movements observed for the NN controller in Fig. 5 are not observed for the case when the NN/RISE control was applied.

B. Scenario II: Obstacle-Ridden Environment

Now, consider stationary and moving obstacles for the wedge formation along with the controller gains outlined earlier along with $K_L = 0.9$, $K_\psi = 1.5$, $\beta_o = 0.5$, and $\kappa = 2$. The robots are initialized so that they must avoid one another while attempting to reach their desired location in the formation.

Fig. 7 shows the formation trajectories in the presence of both stationary and moving obstacles, and examining this figure, it is evident that the robots are able to avoid collisions with
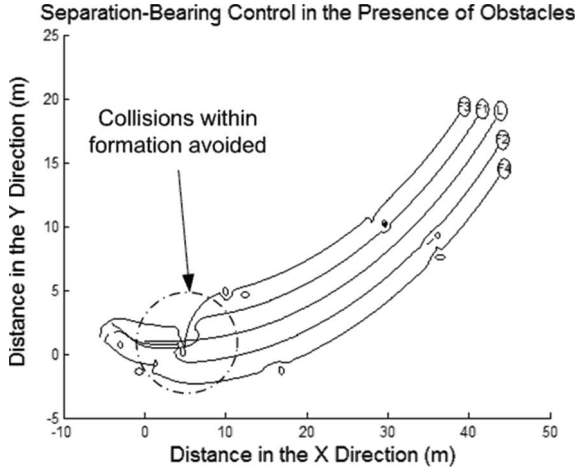
Fig. 7. Formation obstacle avoidance.

their neighbors and maneuver around the encountered obstacles while simultaneously tracking their leaders. Because the followers on the outside of the formation track the robots in the inner formation, the movements of the robots in the interior of the formation propagate to followers on the exterior of the formation. Thus, when a robot on the interior of the formation performs an obstacle avoidance maneuver, their movements are mimicked by their followers, which is evident in Fig. 7. As previously identified, the obstacle avoidance scheme poses potential shortcomings in heavily cluttered environment. However, as shown in Fig. 7, the obstacle avoidance scheme can be effective in undemanding environments as well as ensure that collisions between robots in the formation do not occur.

V. CONCLUSION

In the absence of obstacles, an AS NN tracking controller for leader–follower-based formation control was presented that considers the dynamics of the leader and the followers using backstepping with RISE feedback. The feedback control scheme is valid even when the dynamics of the followers and their leader are unknown since the NN learns them all online. Numerical results were presented, and the asymptotic stability of the system was verified. Simulation results verify the theoretical conjecture and reveal the strength of asymptotic stability over the common result of most NN literature, UUB. The asymptotic stability of the formation in the presence of obstacles was also demonstrated by applying the RISE method to a leader–follower obstacle avoidance scheme. The control was shown to be effective in both static and dynamic obstacle environments, and numerical results were presented. Furthermore, by treating robots in the formation as obstacles, collisions within the formation were guaranteed not to occur. The stability of the system was verified, and the simulation results verified the theoretical conjecture.

Future efforts will address a more comprehensive obstacle avoidance scheme for leader–follower formation control. This work will focus on alleviating the previously observed limitations of the current obstacle avoidance scheme so that multiple objects and more complex environments can be navigated while completing the leader–follower formation control objective.

APPENDIX

Remark A.1: To begin with, certain bounds must be established, and for generality, the subscripts i and j will not be used here. First, bounds on NN quantities will be frequently used as

$$\|W\|_F \leq W_M \qquad \|\sigma\| \leq \sqrt{N_h}$$
$$\|\sigma(1-\sigma)\| \leq \sqrt{N_h} + N_h \qquad \left\|\dot{\hat{W}}\right\|_F \leq F_M\sqrt{N_h}\|e_c\|$$
$$(A1)$$

where $\|e_c\|$ refers to the velocity tracking error, N_h is the constant number of hidden layer neurons, W_M is the upper bound of the ideal NN weights W, and $F_M = \|F\|_F$ is a constant. Next, bounds relating the physical robotic system are written as

$$|\theta| \leq q_M \qquad \|[\bar{v}^T \quad \dot{\bar{v}}^T \quad \ddot{\bar{v}}^T]\| \leq V_M$$
$$\|[\tau^T \quad \dot{\tau}^T]\| \leq T_M \qquad\qquad (A2)$$

where q_M, V_M, and T_M are known constants relating to the physical capabilities of the mobile robot. Additionally, bounds on the velocity control (10) and its derivatives can be established as

$$\left\|[v_c^T \quad \dot{v}_c^T \quad \ddot{v}_c^T \quad \dddot{v}_c^T]\right\| \leq C_4 + C_5\|e\| \qquad (A3)$$

where $\|e\| = \|[e_1 \quad e_2 \quad e_3]\|$ refers to the position and orientation tracking errors, with $C_i, i = 4,5$ being computable constants dependent on (A2), and the selection of the velocity control gains in (10). Since the backward difference equation (18) is utilized to estimate the higher order derivatives of the control velocity (10), the following bound must also be established:

$$\left\|[v_c^T \quad \dot{v}_c^T \quad \ddot{v}_c^T \quad \dddot{\hat{v}}_c^T]\right\| \leq C_6 + C_7\|e\| \qquad (A4)$$

with $C_i, i = 6,7$ being computable constants. Now, the bounds on the derivative of the ideal NN input x_d as well as the derivative of the estimated NN input $\hat{x}_d$ are found to be

$$\|\dot{x}_d\| \leq C_8 + C_9\|e\| \equiv c_1(t)$$
$$\|\dot{\hat{x}}_d\| \leq C_{10} + C_{11}\|e\| \equiv c_2(t) \qquad (A5)$$

with $C_i, i = 8,9,10,11$ being computable constants. The proof of (A5) is straightforward using (A2)–(A4) along with using similar steps described in [20].

Lemma 1: Upper bounds for N_{B1} and N_{B2} in (24) as well as their derivatives can be defined as in (26)–(29).

Proof: Recalling $\|\varepsilon\| \leq \varepsilon_N$, $\|[\dot{\bar{\tau}}_d^T \quad \ddot{\bar{\tau}}_d^T]\| \leq d'_M$ as well as observing (A1) reveal (26). Next, differentiating N_{B1} reveals $\dot{N}_{B1} = \dot{\varepsilon} + \ddot{\bar{\tau}}_d + W^T\tilde{\sigma}$. Then, recalling $\|\dot{\varepsilon}\| \leq \varepsilon'_N$ and again applying the bounds in (A1) reveal $\|\dot{N}_{B1}\| \leq \varepsilon'_N + d'_M + W_M\|\dot{\tilde{\sigma}}\|$, and the bound in (27) follows by observing

$\widetilde{\sigma} = \sigma - \hat{\sigma}$ and applying the chain rule for derivatives written as

$$
\begin{aligned}
\|\dot{\widetilde{\sigma}}\| &\leq (\sqrt{N_h} + N_h) \left(\|\dot{x}_d\| + \|\dot{\hat{x}}_d\| \right) \\
&= (\sqrt{N_h} + N_h)(c_1(t) + c_2(t)) \\
&= (\sqrt{N_h} + N_h)(C_1 + C_2\|e\|)
\end{aligned}
$$

with $C_1 = C_8 + C_{10}$ and $C_2 = C_9 + C_{11}$.

Now, considering N_{B2}, recalling $\widetilde{W} = W - \hat{W}$, and applying (A1) reveal the bound in (28). Finally, differentiating N_{B2} reveals $\dot{N}_{B2} = \dot{\widetilde{W}}^T \hat{\sigma} + \widetilde{W}^T \dot{\hat{\sigma}}$, and observing $\dot{\widetilde{W}} = -\dot{\hat{W}}$, utilizing the NN weight update law (31), and applying (A1) $\dot{N}_{B2}$ are bounded, as shown in (29), with $C_3 = F_M\sqrt{N_h}$.

Lemma 2: Given the auxiliary function

$$
\begin{aligned}
L = r^T \left(N_{B1} + N_{B2} - \beta_1 \mathrm{sgn}(e_c) \right) - e_c^T N_{B2} \\
- \dot{\beta}_1 \|e_c\| - \dot{e}_c^T \beta_2 \mathrm{sgn}(e_c) - \alpha_0 \beta_2 \|e_c\| \quad \text{(A6)}
\end{aligned}
$$

let $\beta_1(t)$ and β_2 be chosen according to (30), and then

$$
\int_0^t L(s)\,ds \leq \gamma \quad \text{(A7)}
$$

where $\gamma = \|e_c(0)\|(\beta_1(0) + \beta_2) - e_c^T(0)N_{B3}(0) \geq 0$, with $N_{B3} = N_{B1} + N_{B2}$.

Proof: Integrating both sides of (A6), substituting (13), and defining $N_{B3} = N_{B1} + N_{B2}$ yield

$$
\begin{aligned}
\int_0^t L\,ds = &\int_0^t \dot{e}_c^T \left(N_{B3} - (\beta_1 + \beta_2)\mathrm{sgn}(e_c) \right) ds \\
&+ \int_0^t \alpha(t) e_c^T \left(N_{B1} + N_{B2}\left(1 - \frac{1}{\alpha(t)} \right) \right. \\
&\left. \qquad\qquad - \beta_1 \mathrm{sgn}(e_c) \right) ds \\
&- \int_0^t \dot{\beta}_1 \|e_c\|\,ds - \int_0^t \alpha_0 \beta_2 \|e_c\|\,ds. \quad \text{(A8)}
\end{aligned}
$$

Using integration by parts, the first term can be written as

$$
\begin{aligned}
\int_0^t &\dot{e}_c^T \left(N_{B3} - (\beta_1 + \beta_2)\mathrm{sgn}(e_c) \right) ds \\
&= e_c^T \left(N_{B3} - (\beta_1 + \beta_2)\mathrm{sgn}(e_c) \right) \big|_0^t \\
&\quad - \int_0^t e_c^T \left(\dot{N}_{B3} - \dot{\beta}_1 \mathrm{sgn}(e_c) \right) ds \quad \text{(A9)}
\end{aligned}
$$

and substituting (A9) into (A8) reveals

$$
\begin{aligned}
\int_0^t L\,ds \leq &\int_0^t \alpha(t)\|e_c\| \left(\|N_{B1}\| + \|N_{B2}\|\left(1 - \frac{1}{\alpha(t)} \right) \right. \\
&\left. \qquad + \frac{\|\dot{N}_{B3}\|}{\alpha(t)} - \beta_1 - \frac{\alpha_0}{\alpha(t)}\beta_2 \right) ds \\
&+ e_c^T \left(N_{B3} - (\beta_1 + \beta_2)\mathrm{sgn}(e_c) \right) \big|_0^t. \quad \text{(A10)}
\end{aligned}
$$

Recalling $\alpha(t) = \alpha_0 + \alpha_1(t)$, substituting the bounds (26)–(29) into (A10), and rearranging allow the terms to be written as

$$
\begin{aligned}
\int_0^t L\,ds \leq &\int_0^t \alpha(t)\|e_c\| \left(\varsigma_1 + \varsigma_2(t)\left(1 - \frac{1}{\alpha(t)} \right) \right. \\
&\left. + \frac{\varsigma_1'(t) + \varsigma_2'(t)}{\alpha(t)} - \beta_1 - \frac{\alpha_0}{\alpha(t)}\beta_2 \right) ds \\
&+ e_c^T N_{B3} \big|_0^t - \|e_c\|(\beta_1 + \beta_2)\big|_0^t. \quad \text{(A11)}
\end{aligned}
$$

Next, observing $\alpha(t) \geq \alpha_0$, $1/\alpha(t) \leq 1/\alpha_0$, and $0 \leq 1 - 1/\alpha(t) < 1$ for $\alpha_0 \geq 1$, (A11) can be rewritten to reveal

$$
\begin{aligned}
\int_0^t L\,ds \leq &\|e_c\|(\varsigma_1 + \varsigma_2(t)) - \|e_c\|(\beta_1(t) + \beta_2) \\
&+ \|e_c(0)\|(\beta_1(0) + \beta_2) - e_c^T(0)N_{B3}(0) \\
&+ \int_0^t \alpha(t)\|e_c\| \left(\varsigma_1 + \varsigma_2(t) + \frac{\varsigma_1'(t) + \varsigma_2'(t)}{\alpha_0} \right. \\
&\left. \qquad\qquad - \beta_1 - \frac{\alpha_0}{\alpha(t)}\beta_2 \right) ds. \quad \text{(A12)}
\end{aligned}
$$

Examining the first term on the right side of (A12), it can be concluded that $\|e_c\|(\varsigma_1 + \varsigma_2(t) - \beta_1(t) - \beta_2) \leq 0$ if

$$
\beta_1(t) + \beta_2 \geq \varsigma_1 + \varsigma_2(t). \quad \text{(A13)}
$$

If the inequality of (A13) is satisfied, then the constant term $\|e_c(0)\|(\beta_1(0) + \beta_2) - e_c^T(0)N_{B3}(0)$ is guaranteed to be greater than zero. Next, the last term in (A12) is less than zero, provided that

$$
\beta_1(t) + \frac{\alpha_0}{\alpha(t)}\beta_2 \geq \varsigma_1 + \varsigma_2(t) + \frac{\varsigma_1'(t) + \varsigma_2'(t)}{\alpha_0}. \quad \text{(A14)}
$$

Finally, by selecting $\beta_1(t) \geq \varsigma_1 + \varsigma_2(t) + (\varsigma_1'(t) + \varsigma_2'(t))/\alpha_0$ and $\beta_2 > 0$, the inequalities of (A13) and (A14) both hold. Through expansion of the bounds in (26)–(29), the gain terms defined in (30) are revealed to be

$$
\begin{aligned}
K_W &= \sqrt{N_h} + C_{10}(\sqrt{N_h} + N_h)/\alpha_0 \\
K_e &= (\sqrt{N_h} + N_h)(C_2 + W_M C_{11})/\alpha_0 \\
K_{ec} &= C_3/\alpha_0 \\
K_{We} &= (\sqrt{N_h} + N_h)C_{11}/\alpha_0 \\
K_\beta &= \varsigma_1 + W_M\sqrt{N_h} \\
&\quad + \left(\varepsilon_N' + d_M' + (\sqrt{N_h} + N_h)(C_1 + W_M C_{10}) \right)\Big/\alpha_0.
\end{aligned}
$$

Remark A.2: In the proof of the following theorems, the subscripts i and j will be reinstated.

Proof of Theorem 1—(Follower Dynamic Control): Consider the following positive-definite Lyapunov candidate:

$$
V_j' = \alpha_{jo}V_j + \Lambda_j V_{j\mathrm{NN}} \quad \text{(A15)}
$$

where $\Lambda_j = k_{j2} + d_j(k_{j2} + k_{j3}) > 0$, $V_j = (k_{j2}/2)(e_{j1}^2 + e_{j2}^2) + (d_j k_{j3}/2)e_{j3}^2$, and

$$V_{j\text{NN}} = \frac{1}{2}e_{jc}^T e_{jc} + \frac{1}{2}r_j^T \overline{M}_j r_j + P_j + Q_j \quad (A16)$$

$$P_j = \|e_{jc}(0)\|(\beta_{j1}(0) + \beta_{j2}) - e_{jc}^T(0)N_{Bj3}(0)$$
$$- \int_0^t L_j(s)ds \quad (A17)$$

$$Q_j = \frac{1}{2}\text{tr}\left\{\widetilde{W}_j^T F_j^{-1} \widetilde{W}_j\right\} \quad (A18)$$

and $L_j(t)$ is defined in (A6). By Lemma 2, it can be concluded that $P_j \geq 0$. Before proceeding, it is important to observe the existence of the functions $U_1(y_j)$ and $U_2(y_j)$ such that

$$U_1(y_j) \leq V_j' \leq U_2(y_j) \quad (A19)$$

where $y_j = [e_j^T \quad e_{jc}^T \quad r_j^T \quad \sqrt{P_j} \quad \sqrt{Q_j}] \in \Re^{n+2(r+1)}$, $U_1(y_j)$ and $U_2(y_j)$ are defined by $U_1(y_j) = \lambda_{j1}\|y_j\|^2$ and $U_2(y_j) = \lambda_{j2}\|y_j\|^2$, respectively, with $\lambda_{j1} = 1/2\min\{\Lambda_j, \Lambda_j \quad \overline{m}_1, \alpha_{jo} \quad k_{j2}, \alpha_{jo}d_j k_{j3}\}$, $\lambda_{j2} = \max\{\Lambda_j, (\Lambda_j/2)\overline{m}_2, \alpha_{jo}k_{j2}, \alpha_{jo}d_j k_{j3}\}$, and $\overline{m}_1$ and $\overline{m}_2$ are known positive constants satisfying

$$\overline{m}_1\|y_j\|^2 \leq y_j^T \overline{M}_j y_j \leq \overline{m}_2\|y_j\|^2.$$

Differentiating V_j and substituting the kinematic error dynamics (12)

$$\dot{V}_j = -k_{j2}k_{j1}e_{j1}^2 - k_{j2}^2 e_{j2}^2 - k_{j3}^2 e_{j3}^2$$
$$+ 2k_{j2}e_{j2}v_i \sin\left(\frac{e_{j3}}{2}\right)\cos\left(\theta_i - \frac{\theta_{jr} + \theta_j}{2}\right)$$
$$- k_{j3}k_{j2}e_{j2}e_{j3} + k_{j2}e_{j1}e_{j4} + d_j(k_{j2}e_{j2} + k_{j3}e_{j3})e_{j5}.$$

Noting that $|\sin(e_{j3}/2)| \leq |e_{j3}|$ for all $e_{j3} \in [-\pi, \pi]$, $\dot{V}_j$ takes the form of

$$\dot{V}_j \leq -k_{j2}k_{j1}e_{j1}^2 - k_{j2}^2 e_{j2}^2 - k_{j3}^2 e_{j3}^2 + k_{j2}|e_{j2}e_{j3}|(k_{j3} + 2v_{i\max})$$
$$+ k_{j2}e_{j1}e_{j4} + d_j(k_{j2}e_{j2} + k_{j3}e_{j3})e_{j5}. \quad (A20)$$

In the next step, it is desired to select k_{j3} such that $(k_{j3} + 2v_{i\max}) < 2k_{j3}$, and for any $\varepsilon_{vi} > 0$, selecting $k_{j3} = 2v_{i\max} + \varepsilon_{vi}$ ensures that this inequality holds. Specifically, we select $\varepsilon_{vi} = 2\varepsilon_{k3}k_{j3}$, where $\varepsilon_{k3} \in (0, 1/2)$ so that $k_{j3} = 2v_{i\max}/(1 - 2\varepsilon_{k3})$, and selecting k_{j3} in this way allows $\dot{V}_j$ to be written as

$$\dot{V}_j \leq -k_{j2}k_{j1}e_{j1}^2 - \varepsilon_{k3}k_{j2}^2 e_{j2}^2 - \varepsilon_{k3}k_{j3}^2 e_{j3}^2$$
$$- (1 - \varepsilon_{k3})(k_{j3}|e_{j3}| - k_{j2}|e_{j2}|)^2$$
$$+ k_{j2}e_{j1}e_{j4} + d_j(k_{j2}e_{j2} + k_{j3}e_{j3})e_{j5}. \quad (A21)$$

Next, differentiating (A16), noting $\dot{P}_j = -L_j$, utilizing the definition of the filtered tracking error (13), and substituting the

filter tracking error dynamics and the derivatives of (A17) and (A18) reveal

$$\dot{V}_{j\text{NN}} = -\alpha_j(t)e_{jc}^T e_{jc} - (k_{js} + 1)r_j^T r_j$$
$$+ r_j^T \widetilde{N}_j + r_j^T(N_{Bj1} + N_{Bj2}) - r_j^T \beta_{j1}(t)\text{sgn}(e_{jc})$$
$$- r_j^T \beta_{j2}\text{sgn}(e_{jc}) - L_j + \text{tr}\left\{\widetilde{W}_j^T F^{-1}\dot{\widetilde{W}}_j\right\}.$$

Then, substitution of the NN weight tuning law (31) and $L_j(t)$ into (A6) reveals

$$\dot{V}_{j\text{NN}} \leq -\alpha_j(t)\|e_{jc}\|^2 - (k_{js} + 1)\|r_j\|^2 + \|r_j\| \|\widetilde{N}_j\|$$
$$+ \left(\|\dot{\beta}_{j1}\| - \alpha_j(t)\beta_{j2}\right)\|e_{jc}\| + \alpha_{j0}\beta_{j2}\|e_{jc}\|. \quad (A22)$$

Recalling $\alpha_j(t) = \alpha_{j0} + \alpha_{j1}(t)$ and selecting $\alpha_{j1}(t) \geq \|\dot{\beta}_{j1}(t)\|/\beta_{j2}$ allow (A22) to be rewritten as

$$\dot{V}_{j\text{NN}} \leq -\alpha_{j0}\|e_{jc}\|^2 - (k_{js} + 1)\|r_j\|^2 + \|r_j\| \|\widetilde{N}_j\|. \quad (A23)$$

Next, combining (A21) and (A23) and completing the squares with respect to e_{j1}, e_{j2}, and e_{j3} yield

$$\dot{V}_j' \leq -\alpha_{j0}\lambda_{j3}\|e_j\|^2 - \alpha_{j0}\lambda_{j4}\|e_{jc}\|^2$$
$$-\Lambda_j(k_{js} + 1)\|r_j\|^2 + \Lambda_j\|r_j\| \|\widetilde{N}_j\|$$

where $\lambda_{j3} = \min(k_{j2}(k_{j1} - 1/2), \varepsilon_{k3}k_{j2}(k_{j2} - d_j/2\varepsilon_{k3}), \varepsilon_{k3}k_{j3}(k_{j3} - d_j/2\varepsilon_{k3})) > 0$, provided that $k_{j1} > 1/2$, $k_{j2} > d_j/(2\varepsilon_{k3})$, and $k_{j3} > d_j/(2\varepsilon_{k3})$, and $\lambda_{j4} = \min(k_{j2}/2 + d_j(k_{j2} + k_{j3}), k_{j2} + d_j(k_{j2} + k_{j3})/2) > 0$. Recalling $k_{j3} = 2v_{i\max}/(1 - 2\varepsilon_{k3})$, the third inequality can be rewritten as $2v_{i\max}/1 - 2\varepsilon_{k3} > d_j/2\varepsilon_{k3}$ or $\varepsilon_{k3} > d_j/(4v_{i\max} + 2d_j)$, and it is worth noting that $\varepsilon_{k3} \in (0, 1/2)$ as required since $v_{i\max} > 0$. Next, completing the square with respect to $\|r_j\|$ and recalling the bound defined in (25), $\dot{V}_j'$ becomes

$$\dot{V}_j' \leq -\alpha_{j0}\lambda_{j3}\|e_j\|^2 - \lambda_{j5}\|z_j\|^2$$
$$- k_{js}\Lambda_j\left(\|r_j\| - \frac{\rho(\|z_j\|)\|z_j\|}{2k_{js}}\right)^2$$
$$+ \frac{\Lambda_j\rho(\|z_j\|)^2\|z_j\|^2}{4k_{js}} \quad (A24)$$

where $\lambda_{j5} = \min(\alpha_{j0}\lambda_{j4}, \Lambda_j)$ and greater than zero, provided that $\alpha_{j0} > 0$. The third term in (A24) is always less than or equal to zero, so consider the first, second, and fourth terms in the following inequality:

$$\dot{V}_j' \leq -\alpha_{j0}\lambda_{j3}\|e_j\|^2 - \left(\lambda_{j5} - \frac{\Lambda_j\rho(\|z_j\|)^2}{4k_{js}}\right)\|z_j\|^2$$
$$\leq -U(y_j) \quad (A25)$$

where $U(y_j) = c\|[e_j^T \quad z_j^T]\|^2$ is a continuous positive-semidefinite function for some real positive constant c defined

on the domain D such that

$$\dot{V}_j' \leq -U(y_j)$$

for

$$D = \left\{ y_j \in \Re^{n+2(r+1)} \middle| \|y_j\| \leq \rho^{-1} \left(\sqrt{4\lambda_{j5} k_{js}/\Lambda_j} \right) \right\}.$$
(A26)

The inequalities in (A19) and (A26) can be used to show that $V_j' < \infty$ and bounded in D, and therefore, e_j, e_{jc}, r_j, P_j, and Q_j are also bounded in D. Continuing this way by observing the boundedness of e_j, e_{jc}, and r_j in D, standard linear analysis methods can be used to prove that all of the quantities in (7), (9)–(11), (13), (14), (20), and (22) are also bounded in D. Therefore, using the definitions for $U(y_j)$ and $z_j(t)$, it can be concluded that $U(y_j)$ is uniformly continuous. For complete details of the steps to draw this conclusion, see [19].

Let $S \subset D$ denote a region of attraction such that

$$S = \left\{ y_j(t) \subset D | U_2(y_j(t)) \right.$$

$$\left. < \lambda_{j2} \left(\rho^{-1} \left(\sqrt{4\lambda_{j5} k_{js}/\Lambda_j} \right) \right)^2 \right\}. \quad \text{(A27)}$$

Applying [21, Theorem 8.4], it can be concluded that $c\|[e_j^T \quad z_j^T]\|^2 \to 0$ as $t \to \infty \; \forall y_j(0) \in S$. Thus, $\|e_j\| \to 0$ as $t \to \infty$, and from the definition of $z_j(t)$, it is clear that $\|e_{jc}\| \to 0$ as $t \to \infty$ for all $y_j(0) \in S$, thus illustrating the asymptotic stability of the tracking errors and the boundedness of the NN weight estimates.

Remark A.3: The region of attraction (A27) can be made arbitrarily large to include a larger set of initial conditions by increasing the gain k_{js}. Also, the boundedness $\hat{W}_j$ does not guarantee that the estimates converge to the ideal W unless certain signals are persistently excited [20].

Proof of Theorem 2—(Leader Stability): Consider the Lyapunov candidate

$$V_i' = \alpha_{i0} V_i + \Lambda_i V_{iNN} \quad \text{(A28)}$$

where $\Lambda_i = 1 + 1/k_{i2}$, $V_i = 1/2(e_{i1}^2 + e_{i2}^2) + 1 - \cos e_{i3}/k_{i2}$, and

$$V_{iNN} = \frac{1}{2} e_{ic}^T e_{ic} + \frac{1}{2} r_i^T \overline{M}_i r_i + P_i + Q_i \quad \text{(A29)}$$

where P_i and Q_i are defined similarly to (A17) and (A18), respectively.

First, taking the derivative of V_i and substituting the error dynamics (32), control velocity (33), and velocity tracking error (34) reveal the following after simplification

$$\dot{V}_i = -k_{i1} e_{i1}^2 - k_{i3} \sin^2 e_{i3} + e_{i1} e_{ic4} + \frac{\sin e_{i3}}{k_{i2}} e_{ic5}. \quad \text{(A30)}$$

Then, examining (A29), one can see that it is defined similarly to the Lyapunov function (A16) defined for follower j. Exploit-

ing these similarities and applying steps and justifications similar to the ones used to derive (A22)–(27), it is straightforward to show that there exist domain D_i and region of attraction S_i such that $\dot{V}_{iNN} \leq -U(y_i)$ and, thus, $\dot{V}_{iNN}$ is uniformly continuous, provided that $k_{i1} > 1/2$ and $k_{i3} > 1/(2k_{i2})$. Therefore, again applying [21, Theorem 8.4], it can be concluded that $c_i\|[e_{i1} \quad e_{i3} \quad z_i^T]\|^2 = c_i\|[e_{i1} \quad e_{i3} \quad e_{ic}^T \quad r_i^T]\|^2 \to 0$ as $t \to \infty \; \forall y_i(0) \in S_i$, where c_i is a positive real constant. Thus, $\|[e_{i1} \quad e_{i3}]\| \to 0$, and from the definition of $z_i(t)$, it is clear that $\|e_{ic}\| \to 0$ as $t \to \infty$ for all $y_i(0) \in S_i$ and, thus, $\dot{V}_{iNN} \to 0$ as $t \to \infty$.

Using the knowledge $\|[e_{i1} \quad e_{i3}]\| \to 0$ and examining (31) and the definition of e_{ic}, it is then straightforward to verify that $e_{i2} \to 0$ as $t \to \infty$. Thus, the asymptotic stability of the position and velocity tracking errors and the boundedness of the NN weight estimates for leader i follow.

Proof of Theorem 3—(Formation Stability): Consider the following Lyapunov candidate

$$V_{ij} = \sum_1^N V_j' + V_i' \quad \text{(A31)}$$

where V_j' is defined in (A15) and V_i' is defined in (A28). Taking the derivative of (A31) yields $\dot{V}_{ij} = \sum_1^N \dot{V}_j' + \dot{V}_i'$, and using the results of *Theorems 1* and *2*, there exists a region of attraction S_{ij} defined similarly to (A27) such that the positions, orientation, and velocity tracking errors for the entire formation are AS and that the NN weights remain bounded.

Lemma 3: If β_{jo} is chosen according to (45) so that $\beta_{jo} \geq \zeta_M + (1/\kappa)\zeta_M'$, then

$$\int_0^t R_j(s) ds \leq \beta_{jo} \|e_{jo}(0)\| - e_{jo}^T(0)\zeta_j(0). \quad \text{(A32)}$$

Proof: Define $R_j(t) = \vartheta_j^T(\zeta_j - \beta_{jo}\text{sgn}(e_{jo}))$. Integrating both sides and using (38) yield

$$\int_0^t R_j(s) ds = \int_0^t \kappa e_{jo}(\zeta_j - \beta_{jo}\text{sgn}(e_{jo})) \, ds$$

$$+ \int_0^t \dot{e}_{jo}(\zeta_j - \beta_{jo}\text{sgn}(e_{jo})) \, ds. \quad \text{(A33)}$$

Then, applying integration by parts to the second term on the right side of (A33) reveals

$$\int_0^t R_j(s) ds \leq e_{jo}^T(t)\zeta_j(t) - \beta_{jo}\|e_{jo}(t)\|$$

$$+ \beta_{jo}\|e_{jo}(0)\| - e_{jo}^T(0)\zeta_j(0)$$

$$+ \int_0^t \kappa\|e_{jo}\| \left(\|\zeta_j\| + \frac{1}{\kappa} \|\zeta_j'\| - \beta_{jo} \right) ds.$$
(A34)

Recalling $\|\zeta_j\| \leq \zeta_M$ and $\|\zeta_j'\| \leq \zeta_M'$ and selecting β_{jo} according to (45), the inequality of (A32) follows.

Proof of Theorem 4—(Follower Obstacle Avoidance): Consider the Lyapunov candidate $V'_{jo} = \alpha_{j0}V_{jo} + \Lambda_{jo}V_{jNN}$, where $\Lambda_{jo} = 1 + d_j$, $V_{jo} = (1/2)e_{jo}^T e_{jo} + (1/2)\vartheta_j^T\vartheta_j + \Gamma_j$, V_{jNN} as defined in (A16), with e_{jc} and r_j being replaced by e_{jco} and r_{jo}, respectively, and $\Gamma_j = \beta_{j3}\|e_{jo}(0)\| - e_{jo}^T(0)\zeta_j(0) - \int_0^t R_j(s)ds$. By *Lemma 3*, it can be concluded that $\Gamma_j \geq 0$. Taking the time derivative of V_{jo} and utilizing (42) and (47) yield

$$\dot{V}_{jo} = e_{jo}^T\vartheta_j - \kappa e_{jo}^T e_{jo} - G\vartheta_j^T\vartheta_j + \vartheta_j^T E_j e_{jco}. \quad (A35)$$

Noting that $e_j^T\vartheta_j \leq (1/2)(e_j^T e_j + \vartheta_j^T\vartheta_j) \leq e_j^T e_j + \vartheta_j^T\vartheta_j$ and using the definition of E_j in (45), (A35) can be rewritten as

$$\dot{V}_{jo} \leq -(\kappa - 1)e_{jo}^T e_{jo} - (G - 1)\vartheta_j^T\vartheta_j$$
$$+ \vartheta_{j1}e_{jco4} + d_j\vartheta_{j2}e_{jco5}. \quad (A36)$$

Then, differentiating V_{jNN} and applying steps and justifications similar to the ones used to derive (A22)–(A27), except completing the squares with respect to ϑ_j instead of e_j, it is straightforward to show the asymptotic stability of the position and velocity tracking errors and the boundedness of the NN weight estimates, provided that $\kappa > 1$ and $G > 1 + (1/2)\max(1, d_j)$.

REFERENCES

[1] Y. Q. Chen and Z. Wang, "Formation control: A review and a new consideration," in *Proc. IEEE Int. Conf. Intell. Robots Syst.*, Aug. 2005, pp. 3181–3186.

[2] G. L. Mariottini, G. Pappas, D. Prattichizzo, and K. Daniilidis, "Vision-based localization of leader–follower formations," in *Proc. IEEE Eur. Control Conf. Decision Control*, Dec. 2005, pp. 635–640.

[3] J. P. Desai, J. Ostrowski, and V. Kumar, "Controlling formations of multiple mobile robots," in *Proc. IEEE Int. Conf. Robot. Autom.*, May 1998, pp. 2864–2869.

[4] J. Shao, G. Xie, J. Yu, and L. Wang, "A tracking controller for motion coordination of multiple mobile robots," in *Proc. IEEE Int. Conf. Intell. Robots Syst.*, Aug. 2005, pp. 783–788.

[5] H. Hsu and A. Liu, "Multi-agent based formation control using a simple representation," in *Proc. IEEE Int. Conf. Netw., Sens. Control*, Mar. 2004, pp. 276–281.

[6] X. Li, J. Xiao, and Z. Cai, "Backstepping based multiple mobile robots formation control," in *Proc. IEEE Int. Conf. Intell. Robots Syst.*, Aug. 2005, pp. 887–892.

[7] S. Mastellone, D. Stipanović, C. Graunke, K. Intlekofer, and M. Spong, "Formation control and collision avoidance for multi-agent non-holonomic systems: Theory and experiments," *Int. J. Rob. Res.*, vol. 27, no. 1, pp. 107–126, Jan. 2008.

[8] Y. Li and X. Chen, "Dynamic control of multi-robot formation," in *Proc. IEEE Int. Conf. Mechatronics*, Jul. 2005, pp. 352–357.

[9] M. Breivik, M. Subbotin, and T. Fossen, "Guided formation control for wheeled mobile robots," in *Proc. IEEE Int. Conf. Robot. Autom.*, Dec. 2006, pp. 1–7.

[10] Y. Liang and H. Lee, "Decentralized formation control and obstacle avoidance for multiple robots with nonholonomic constraints," in *Proc. IEEE Am. Control Conf.*, Jun. 2006, pp. 5596–5601.

[11] H. Takahashi, H. Nishi, and K. Ohnishi, "Autonomous decentralized control for formation of multiple mobile robots considering ability of robot," *IEEE Trans. Ind. Electron.*, vol. 51, no. 6, pp. 1272–1279, Dec. 2004.

[12] C. De La Cruz and R. Carelli, "Dynamic modeling and centralized formation control of mobile robots," in *Proc. IEEE Conf. Ind. Electron.*, Nov. 2006, pp. 3880–3885.

[13] K. D. Do, "Formation tracking control of unicycle-type mobile robots with limited sensing ranges," *IEEE Trans. Control Syst. Technol.*, vol. 16, no. 3, pp. 527–538, May 2008.

[14] T. Dierks and S. Jagannathan, "Control of nonholonomic mobile robot formations: Backstepping kinematics into dynamics," in *Proc. IEEE Int. Conf. Control Appl.*, Oct. 2007, pp. 94–99.

[15] T. Dierks, "Nonlinear control of nonholonomic mobile robot formations," M.S. thesis, Univ. Missouri—Rolla, Rolla, MO, 2007. [Online]. Available: http://scholarsmine.mst.edu

[16] S. S. Ge and C. H. Fua, "Queues and artificial potential trenches for multirobot formations," *IEEE Trans. Robot.*, vol. 21, no. 4, pp. 646–656, Aug. 2005.

[17] P. Ogren and N. E. Leonard, "Obstacle avoidance in formation," in *Proc. IEEE Conf. Robot. Autom.*, Sep. 14–19, 2003, pp. 2492–2497.

[18] B. Xian, M. S. de Queiroz, and D. M. Dawson, "A continuous control mechanism for uncertain nonlinear systems in optimal control," in *Stabilization and Nonsmooth Analysis*. Heidelberg, Germany: Springer-Verlag, 2004, pp. 251–262.

[19] P. M. Patre, W. E. Dixon, K. Kaiser, and W. MacKunis, "Asymptotic tracking for uncertain dynamic systems via a multilayer NN feedforward and RISE feedback control structure," in *Proc. IEEE Am. Control Conf.*, Jul. 2007, pp. 5989–5994.

[20] F. L. Lewis, S. Jagannathan, and A. Yesilderek, *Neural Network Control Of Robot Manipulators and Nonlinear Systems*. London, U.K.: Taylor & Francis, 1999.

[21] H. K. Khalil, *Nonlinear Systems*, 3rd ed. Englewood Cliffs, NJ: Prentice–Hall, 2002.

[22] O. Khatib, "Real-time obstacle avoidance for manipulators and mobile robots," *Int. J. Rob. Res.*, vol. 5, no. 1, pp. 90–98, 1986.

[23] R. Fierro and F. L. Lewis, "Control of a nonholonomic mobile robot using neural networks," *IEEE Trans. Neural Netw.*, vol. 9, no. 4, pp. 589–600, Jul. 1998.

Travis Dierks (S'07) received the B.S. and M.S. degrees in electrical engineering from Missouri University of Science and Technology (formerly University of Missouri—Rolla), Rolla, in 2005 and 2007, respectively, where he is currently working toward the Ph.D. degree in the Department of Electrical and Computer Engineering.

His research interests include nonlinear control, neural network control, and the control and coordination of autonomous ground and aerial vehicles.

Mr. Dierks is a GAANN Fellow.

S. Jagannathan (S'89–M'95–SM'99) received the B.S. degree in electrical engineering from the College of Engineering, Guindy, Anna University, Madras, India, in 1987, the M.S. degree in electrical engineering from the University of Saskatchewan, Saskatoon, SK, Canada, in 1989, and the Ph.D. degree in electrical engineering from the University of Texas, Arlington, in 1994.

From 1986 to 1987, he was a Junior Engineer with Engineers India Ltd., New Delhi, India. From 1990 to 1991, he was a Research Associate and Instructor with the University of Manitoba, Winnipeg, MB, Canada. From 1994 to 1998, he was a Consultant with the Systems and Controls Research Division, Caterpillar Inc., Peoria, IL. From 1998 to 2001, he was with the University of Texas, San Antonio. Since September 2001, he has been with Missouri University of Science and Technology (formerly University of Missouri—Rolla), Rolla, where he is currently Rutledge-Emerson Distinguished Professor and Site Director for the NSF Industry/University Cooperative Research Center on Intelligent Maintenance Systems. He has coauthored more than 220 refereed conference and juried journal articles and several book chapters and three books entitled *Neural Network Control of Robot Manipulators and Nonlinear Systems* (Taylor & Francis, 1999), *Discrete-Time Neural Network Control of Nonlinear Discrete-Time Systems*, (CRC Press, 2006), and *Wireless Ad Hoc and Sensor Networks: Performance, Protocols and Control* (CRC Press, 2007). He is the holder of 20 patents with several pending. His research interests include adaptive and neural network control, computer/communication/sensor networks, prognostics, and autonomous systems/robotics.

Dr. Jagannathan has served on a number of IEEE conference committees at various capacities and is currently serving on a few conferences. He is an Associate Editor for the IEEE TRANSACTIONS ON NEURAL NETWORKS, IEEE TRANSACTIONS ON CONTROL SYSTEMS TECHNOLOGY, and IEEE SYSTEMS JOURNAL.